# NATIONAL ADVISORY COMMITTEE FOR AERONAUTICS

**TECHNICAL NOTE 3858**

## A LOW-SPEED EXPERIMENTAL INVESTIGATION OF THE EFFECT OF A SANDPAPER TYPE OF ROUGHNESS ON BOUNDARY-LAYER TRANSITION

By Albert E. von Doenhoff and Elmer A. Horton

Langley Aeronautical Laboratory
Langley Field, Va.

Corrected Copy

NACA

Washington
October 1956

A

NATIONAL ADVISORY COMMITTEE FOR AERONAUTICS

TECHNICAL NOTE 3858

# A LOW-SPEED EXPERIMENTAL INVESTIGATION OF THE EFFECT OF A SANDPAPER TYPE OF ROUGHNESS ON BOUNDARY-LAYER TRANSITION

By Albert E. von Doenhoff and Elmer A. Horton

## SUMMARY

An investigation was made in the Langley low-turbulence pressure tunnel to determine the effect of size and location of a sandpaper type of roughness on the Reynolds number for transition. Transition was observed by means of a hot-wire anemometer located at various chordwise stations for each position of the roughness. These observations indicated that when the roughness is sufficiently submerged in the boundary layer to provide a substantially linear variation of boundary-layer velocity with distance from the surface up to the top of the roughness, turbulent "spots" begin to appear immediately behind the roughness when the Reynolds number based on the velocity at the top of the roughness and the roughness height exceeds a value of approximately 600.

At Reynolds numbers even slightly below the critical value (value for transition), the sandpaper type of roughness introduced no measurable disturbances into the laminar layer downstream of the roughness. The extent of the roughened area does not appear to have an important effect on the critical value of the roughness Reynolds number.

## INTRODUCTION

An extensive correlation of transition data for individual three-dimensional roughness particles was made by Loftin in reference 1. This correlation was made in terms of a local roughness Reynolds number based on the roughness height and the velocity at the top of the roughness, a form suggested by Schiller in reference 2 and employed by Tani in reference 3. Reasonably consistent values of the critical roughness Reynolds number were obtained by Loftin in reference 1, so long as the roughness was sufficiently submerged in the boundary layer to provide a velocity variation that was substantially linear with distance from the surface up to a height equal to the height of the roughness. Schwartzberg and Braslow in reference 4 showed that this critical value of the roughness

Reynolds number was not greatly increased, even when the boundary layer was stabilized to small two-dimensional disturbances by the application of area suction. Similar correlations were obtained by Klebanoff, Schubauer, and Tidstrom (ref. 5).

The difference in character for transition as caused by three-dimensional roughness (spheres cemented to the surface) from that caused by two-dimensional roughness (full-span cylindrical wire laid on the surface parallel to the leading edge) is clearly shown by Klebanoff, Schubauer, and Tidstrom in reference 5. Most of the recent data dealing with the effects of two-dimensional roughness on boundary-layer transition have been summarized by Dryden (ref. 6) for the case of zero pressure gradient in the form of curves of the ratio of the transition Reynolds number in the presence of roughness to the transition Reynolds number for the model smooth plotted against the ratio of the height of the roughness to the boundary-layer thickness. In this type of plot, the assumption is made that transition will occur some distance downstream of the roughness and will gradually approach the roughness position as the Reynolds number is increased.

The data of reference 1 suggested, and those of reference 5 confirmed, the conclusion that three-dimensional roughness elements either had no effect on the boundary layer (subcritical condition) or, within a very narrow range of either speed or height of roughness, caused transition to move substantially up to the element itself.

A remaining problem is the question of the proper criterion for the effects of roughness when interaction between the elements is a possibility, as, for example, in the case of randomly distributed roughness. Such randomly distributed roughness corresponds to the practical case where the leading edge of the wing may in effect become sand blasted or covered with a sandpaper type of roughness. In this connection, it may be noted that the results of tests of airfoils with roughened leading edges (refs. 7 and 8) appeared to indicate the possibility that such roughness would have an effect on the airfoil characteristics only when the Reynolds number based on the roughness height and the free-stream velocity exceeded a critical value which seemed to be independent of the roughness size and the size and shape of the airfoil. It is not apparent that such a criterion is consistent with the concept of a constant critical value of the local roughness Reynolds number based on the velocity at the top of the roughness.

The present experiments were carried out for the purpose of determining the transition-triggering characteristics of such three-dimensional roughness particles when the roughness particles are randomly distributed in a close pattern such as in a sandpaper type of roughness, as well as of examining the relation between the two previously mentioned three-dimensional roughness criteria. It was also desired to obtain the

necessary experimental information in such a way as to show the details of the transition phenomenon more clearly than would be indicated by time averaged velocity or total-pressure boundary-layer measurements.

The investigation was made in the Langley low-turbulence pressure tunnel at Mach numbers ranging from 0.15 to 0.25 by use of an 85-inch-chord NACA $65_{(215)}$-114 airfoil section that completely spanned the 36-inch-wide test section. This airfoil is the same model on which extensive laminar flow studies were reported in reference 9. The occurrence of transition at various chordwise positions for each roughness position was determined by means of a hot-wire anemometer. A great many qualitative indications of the nature of the flow in the boundary layer, as well as a few quantitative measurements of the level of the velocity fluctuations in the boundary layer, were obtained by this method.

## SYMBOLS

| | |
|---|---|
| $y$ | distance normal to surface of airfoil |
| $\delta$ | total boundary-layer thickness where $\frac{u}{U} = 1.0$ in the Kármán-Pohlhausen method |
| $k$ | height of projection |
| $c$ | chord of airfoil |
| $x$ | distance from airfoil leading edge measured along the chord |
| $s$ | distance from airfoil forward stagnation point measured along the airfoil surface |
| $U_\infty$ | free-stream velocity |
| $U$ | local velocity just outside boundary layer |
| $u$ | local streamwise component of velocity inside boundary layer |
| $u_k$ | value of $u$ at top of roughness projection |
| $u'$ | root-mean-square value of the streamwise component of fluctuating velocity |
| $q_\infty$ | free-stream dynamic pressure |

$\nu$ coefficient of kinematic viscosity

$R_c$ airfoil Reynolds number based on chord and free-stream velocity, $U_\infty c/\nu$

$R_k$ projection Reynolds number based on roughness height and velocity at the top of the roughness, $u_k k/\nu$

$R_{k,\infty}$ projection Reynolds number based on roughness height and free-stream velocity, $U_\infty k/\nu$

$R'$ Reynolds number per foot of chord based on free-stream velocity, $U_\infty/\nu$

$R_\theta$ Reynolds number based on momentum thickness $\theta$ and local velocity

$\theta$ momentum thickness of the boundary layer, $\int_0^\infty \frac{u}{U}\left(1 - \frac{u}{U}\right)dy$

Subscripts:

t Reynolds number at which transition takes place

min minimum value

## APPARATUS AND TESTS

The tests were made in the Langley low-turbulence pressure tunnel on an 85-inch-chord NACA $65_{(215)}$-114 airfoil section (fig. 1), which completely spanned the 36-inch width of the test section. The turbulence level of the tunnel at the speeds involved in this investigation is only a few hundredths of 1 percent. A description of the tunnel is given in reference 10 and a detailed description of the model is given in reference 11. The surface finish of the model was such that laminar flow could be maintained to the 50-percent-chord point up to a Reynolds number of $14 \times 10^6$, a value substantially the same as that obtained previously in references 9 and 11 with the same model.

The pressure distribution of the model was measured from the leading edge region back to approximately 65 percent of the chord by means of 0.008-inch-diameter pressure orifices drilled into the surface. Particular care was taken to provide numerous orifices near the leading edge

so that the location of the forward stagnation point could be accurately determined. The nondimensional velocity distribution calculated from the measured pressure distribution along the upper surface is presented in figure 2.

The appearance of transition was determined by use of a hot-wire anemometer using a platinum iridium wire of 0.0003-inch diameter and of 3/32-inch length. Figures 3 and 4 are photographs of the hot-wire holder. The output from the hot-wire anemometer was fed into an oscilloscope and the traces on the cathode-ray tube were recorded on 35 millimeter film by a special camera setup. The traces thus recorded were correlated with the tunnel velocity, wire position, and roughness location. The type of wire used in this investigation was one which was sensitive only to variations in the u-component of velocity. The wire was compensated for heat-capacity lag at one test condition, and this compensation setting was used for all observations. The cutoff frequency of the amplifier was about 12,000 cycles.

The tests were made with the leading edge of 1/4-inch roughness strips 1 inch in span (fig. 4) located along the center line of the model at various positions from $\frac{1}{4}$ inch to $6\frac{1}{4}$ inches from the forward stagnation point measured along the surface and for full-span area-distributed roughness (fig. 1) from the forward stagnation point to 6 inches and to 12 inches back of the forward stagnation point. The roughness in all cases was provided by an application of either No. 60 or No. 120 carborundum grains, of grit sizes that met the specifications of reference 12. The grains were thinly spread over the surface to cover 5 to 10 percent of the surface area and were cemented by a thin coating of shellac applied before the roughness grains were spread. A closeup of the roughness as applied to the model is presented as figure 5.

In general, the No. 60 and No. 120 carborundum particles projected above the surface about 0.011 inch and 0.005 inch, respectively; however, the maximum particle height in each patch is also of interest. During the course of the investigation, although each roughness patch was examined carefully with the unaided eye, the height of the particles was not measured. Following completion of the tests, a series of ten patches 1/4 inch by 1 inch of both sizes of grain were applied to a surface in the same manner used in applying the grains to the airfoil surface, and each of these patches was examined with a 15-power shop microscope to determine the actual particle height. The results of this examination are shown in figure 6, which shows the probability of finding at least one roughness particle of a given height in one patch of roughness. The curves of figure 6 show that, for No. 120 carborundum grain of 0.005-inch nominal size, it is virtually certain that each patch would have at least one particle projecting 0.008 inch above the surface, and about 50 percent of the patches would have at least one particle 0.009 inch high, whereas the chances of finding a particle 0.012 inch high would be very

small. Similarly, for the No. 60 carborundum of 0.011-inch nominal size, it is virtually certain that every patch will contain at least one particle 0.016 inch high and approximately 50 percent of the patches will have at least one particle 0.018 inch high, whereas the chances of finding a particle 0.021 inch high in any patch is very small. The probable maximum height of a particle for No. 120 carborundum is therefore taken as 0.009 inch, and the probable maximum height of a particle for No. 60 carborundum is taken as 0.018 inch.

For each position of roughness, the hot-wire measurements were made at a sufficient number of chordwise positions back of the roughness to make possible determination of a curve of Reynolds number for transition as a function of chordwise position of the wire.

Some of the preliminary measurements were made with full-span strips of roughness 1/4-inch wide. The relatively narrow width of the strip was chosen in order to permit correlation of transition with local boundary-layer conditions. When these measurements were made, it was found that, occasionally, the first indications of transition were obtained at a substantially lower tunnel speed for a downstream position than for more forward positions. In each such case, reexamination of the strip of roughness showed one or more particles in an off-center location projecting above the general level of the roughness. Because of the manner in which turbulent flow spreads, such unusually high projections affected the downstream observations but not the upstream ones. In order to facilitate inspection of the strip of roughness, its spanwise extent was reduced to 1 inch. Such small roughness strips were removed and reapplied two or more times, and the initial appearance of turbulence in each case occurred at very nearly the same Reynolds number; these results indicated that such roughness strips could be satisfactorily duplicated.

## BOUNDARY-LAYER CALCULATIONS

In order to correlate the occurrence of transition with local boundary-layer conditions, it is of course necessary to know the velocity distribution in the boundary layer for all locations at which the roughness is placed. These laminar boundary-layer characteristics were calculated according to the method outlined in reference 13, that is, essentially by the Kármán-Pohlhausen method as modified by Walz (ref. 13, ch. 12, sec. B). This method is summarized in this section.

The momentum thickness $\theta$ of the boundary layer may be computed from the following equation:

$$\left(\frac{\theta}{c}\sqrt{R_c}\right)^2 \equiv \Theta^2 = \frac{0.470}{\left(\frac{U}{U_\infty}\right)^6}\int_0^{s/c}\left(\frac{U}{U_\infty}\right)^5 d\left(\frac{s}{c}\right) \tag{1}$$

The velocity distribution in the boundary layer may be obtained as follows: The form parameter $K$ is defined as $\frac{\theta^2}{\nu}\frac{dU}{dx}$ or as

$$K \equiv \Theta^2 \frac{d\left(\frac{U}{U_\infty}\right)}{d\left(\frac{x}{c}\right)} \tag{2}$$

The form parameter $K$ is related to the Pohlhausen shape parameter $\lambda = \frac{\delta^2}{\nu}\frac{dU}{dx}$ as follows

$$K = \left(\frac{37}{315} - \frac{\lambda}{945} - \frac{\lambda^2}{9072}\right)^2\lambda \tag{3}$$

The parameter $\lambda$ may also be written as

$$\lambda \equiv \Delta^2 \frac{d\left(\frac{U}{U_\infty}\right)}{d\left(\frac{x}{c}\right)} \tag{4}$$

where

$$\Delta \equiv \frac{\delta}{c}\sqrt{R_c}$$

Equation (3) is then solved for $\lambda$, and the velocity distribution in the boundary layer may be obtained by using the following expression

$$\frac{u}{U} = F(\eta) + \lambda G(\eta) \tag{5}$$

where

$$\eta \equiv \frac{y}{\delta}$$

$$F(\eta) \equiv 2\eta - 2\eta^3 + \eta^4$$

$$G(\eta) \equiv \frac{1}{6}\eta(1 - \eta)^3$$

The measured velocity distribution over the airfoil used in these calculations is presented in figure 2. The boundary-layer parameters $\lambda$ and $\Delta$ were calculated by the use of the aforementioned relations and the measured velocity distribution. The shape parameter $\lambda$ is plotted against $s/c$ in figure 7, and the nondimensional boundary-layer thickness $\Delta$ or $\frac{\delta}{c}\sqrt{R_c}$ as a function of $s/c$ is given in figure 8. In order to facilitate the calculations involved in the analysis of the data, the nondimensional velocity distribution $u/U_\infty$ is also presented in figure 9 as a function of $\frac{y}{c}\sqrt{R_c}$ for various chordwise positions.

## RESULTS AND DISCUSSION

Hot-wire traces of the time variation of velocity in the boundary layer as observed for various locations of the roughness are shown in figure 10. For each location of roughness, observations were made at various positions downstream throughout the range of speed necessary to include the transition phenomena at the point of observation. To the left of each hot-wire trace is a short tick which indicates the corresponding value of the Reynolds number per foot of chord as read on the vertical scale of the figure. The chordwise location of the point of observation of each group of hot-wire traces is indicated at the bottom of the figure, as is the height of the wire above the surface in thousandths of an inch. Also shown in the figure is the time scale for the traces. Time increases from left to right. It should be noted that the amplifier gain setting for the traces shown in figure 10(a) was the same for all traces. This procedure resulted in substantially a straight line for the laminar traces. In parts (b), (c), (d), (e), and (f) of figure 10, however, the amplifier gain was increased for the conditions corresponding to completely laminar flow, and the traces for this condition, therefore, show some velocity fluctuations. These fluctuations, however, are of a completely different character from those corresponding to turbulent flow.

In general, transition appears to start as disturbances of very short duration that occur comparatively infrequently at a position just behind the roughness. As the position of observation moves downstream and the speed is kept constant, the frequency of the turbulent bursts does not appear to change, but the duration of each burst becomes longer. This phenomenon is shown very clearly in figure 10(b) at a Reynolds number of $0.44 \times 10^6$. Figure 10 also shows that each burst of turbulence is followed by a condition termed by Schubauer and Klebanoff (ref. 14) as a "logarithmic decrement" type of velocity variation. The increase in duration of individual bursts with distance downstream of the roughness is consistent with the description of the origin of transition given in reference 14; that is, it is consistent with the concept of transition beginning as turbulent spots that start in the vicinity of the roughness and grow as they move downstream.

A quantitative summary of the data of figure 10 is given by the data presented in figure 11. Each part of figure 11 consists essentially of a pair of curves. The lower curve of each pair gives approximately the lowest value of the Reynolds number per foot at which any turbulent bursts were observed for a given location of the roughness plotted against the observation position. The upper curve gives the maximum value of the Reynolds number per foot at which any traces of laminar flow could be detected. In other words, for conditions corresponding to the lower curve, the flow was nearly always laminar, and for those corresponding to the upper curve, the flow was nearly always turbulent. Examination of the various parts of figure 11 indicates that the lowest speed at which any turbulent flow could be found was substantially independent of the position of observation. This is generally true except for the most forward observation positions where, because of the extremely short duration of the bursts, they were difficult to observe and, as a result, these points may be plotted at too high a value of the unit Reynolds number.

The value of the speed at which the flow is nearly completely turbulent decreases appreciably as the point of observation moves downstream for the more forward roughness locations (figs. 11(a) and (b)). This trend is as would be expected if turbulence began as a series of turbulent bursts originating at or near the roughness and increasing in size as they moved downstream. For the more downstream positions of the roughness (figs. 11(c) to 11(f)), the upper and lower curves almost coalesce; that is, the speed range between fully laminar and fully turbulent flow almost vanishes. The data on which figure 11 is based include many more observations than those presented in figure 10, which are merely representative samples of the oscilloscope records.

Quantitative observations of the root-mean-square values of the fluctuations were made both with and without roughness through the speed range corresponding to that for which turbulence occurred when roughness was present. Typical examples of these measurements are presented in figure 12 as functions of the free-stream velocity. From figure 12, it is seen that the root-mean-square level of fluctuations in the laminar boundary layer, even at positions as far downstream as 50 percent of the chord, is as low on the airfoil with roughness present as on the smooth airfoil. It thus appears that, at speeds below those at which turbulent bursts occur, the presence of the roughness does not result in any measurable disturbance in the boundary layer that would hasten transition. It is therefore to be presumed that, at speeds below the critical speed for the roughness, no upstream movement of the transition region would occur even if the model were sufficiently long for transition to occur naturally in the region of favorable pressure gradient.

This type of phenomenon, therefore, appears to be strongly contrasted to the manner in which transition occurs when it is caused by two-dimensional disturbances. The data for the two-dimensional type of disturbance have been summarized in reference 6. This summary indicates that, for the case of two-dimensional disturbances, the roughness introduces into the boundary layer a measurable disturbance which grows until transition occurs.

If, as seems likely from an examination of the oscillograph records (see fig. 10), transition associated with the type of roughness of the present investigation results from the formation of discrete eddies or disturbances originating at the roughness particles, it should be possible to relate the occurrence of such disturbances to the characteristics of local flow about the roughness. That is, if all the roughness particles are regarded as being geometrically similar, and if the roughness is regarded as being sufficiently submerged in the boundary layer to provide substantially linear velocity variation from the surface to the top of the roughness, discrete eddies should form when the Reynolds number of the flow about the roughness reaches a critical value. This concept is not new; it was proposed by Schiller (ref. 2) and used by Loftin in analyzing the data presented in reference 1.

This view is supported by the data presented in figure 13, which is a plot of the critical Reynolds number $R_{k,t}$ based on the height of the roughness and the velocity at the top of the roughness as a function of the chordwise position of the roughness. The velocity at the top of the roughness was found either from the theoretical boundary-layer calculations previously described or, if the roughness projected completely through the boundary layer, from the measured pressure distribution. For all roughness positions more than 0.025c from the forward stagnation point, the critical roughness Reynolds number $R_{k,t}$ was substantially constant within rather close limits. For positions nearer the forward stagnation point than 0.025c, the critical roughness Reynolds number $R_{k,t}$ increased markedly. It is to be noted that, for positions nearer the forward stagnation point than 0.025c, the roughness protruded nearly through the boundary layer, and, for the three positions closest to the forward stagnation point, the roughness protruded completely through the boundary layer. (See fig. 14.) It is entirely possible that for the range of conditions of the present tests, the boundary layer over the region of the airfoil in the vicinity of the forward stagnation point was sufficiently stable to cause small eddies originating at the roughness to be damped out before they travelled downstream far enough to affect the less stable laminar boundary layer farther downstream. At any rate, these results indicate that if the height of the roughness particle is so small that the roughness Reynolds number is less than 600 based on maximum particle size or less than 250 based on nominal particle size, the roughness is not large enough to cause transition. This statement appears to be valid even for roughness heights several times the boundary-layer thickness. The order of magnitude of the critical roughness Reynolds number is within the range of those found by Loftin (ref. 1) and is not much different from the value found by Schwartzberg and Braslow (ref. 4).

The extent of the roughened area does not appear to have an important effect on the height of roughness necessary to cause transition. When the grains of roughness were spread from the leading edge to 6 inches or

12 inches back of the leading edge (fig. 1), the airfoil Reynolds number at which transition occurred was substantially the same as for a spot of roughness 1 inch in span and 1/4 inch in chord located from 2 to $2\frac{1}{4}$ inches from the forward stagnation point. This location (that is, the position at which, for given free-stream conditions, the value of the roughness Reynolds number $R_k$ was a maximum) was approximately the most critical location for the height of roughness used.

## APPLICATION OF RESULTS

An examination of the consequences of the inference drawn from the preceding discussion, namely, that transition occurs when the local roughness Reynolds number $R_k$ exceeds a value of 600, is of interest. The nature of these consequences will be examined with particular reference to the airfoil studied in the present investigation by calculating the critical conditions for various heights of roughness. Figure 15 shows the variation of the roughness Reynolds number $R_k$ for 0.018-inch roughness particles with position along the surface for several values of the airfoil Reynolds number. The roughness position for maximum $R_k$ does not vary rapidly with airfoil Reynolds number and occurs when the height of the roughness is slightly less than the total boundary-layer thickness. For far forward roughness positions, $R_k$ is low because of the low value of the potential flow velocity near the forward stagnation point. For far rearward roughness positions, $R_k$ is low because the roughness is deeply buried in the boundary layer.

Several sets of calculations of this nature were made for different heights of roughness. The results are summarized in figures 16 and 17. For each height of roughness, the position along the surface corresponding to a maximum value of $R_k$ was found, and the value of $R_c$ corresponding to a value of $R_k$ of 600 at this location was then calculated. This value of $R_c$ is the smallest value at which a value of $R_k$ of 600 can be obtained with the roughness of a given height situated at any position along the surface. Figure 16 gives the relation between the minimum critical airfoil Reynolds number and the most sensitive location of the roughness, with the height of the roughness as a parameter for a fixed value of the critical roughness Reynolds number of 600. Figure 17 plots the same information in a slightly different manner. Here the minimum value of the critical airfoil Reynolds number for a roughness Reynolds number $R_{k,t}$ of 600 for roughness situated at the most sensitive location is plotted against the ratio of the roughness height to airfoil chord. From figure 17, it is seen that the curve of $R_{c,min}$ for $R_{k,t} = 600$, when plotted as a function of $k/c$ on log log paper, is nearly a straight line with a slope of -1. This result, of course, indicates that $R_{k,\infty}$, which

is the product of $k/c$ and $R_{c,min}$, is approximately constant and equal to about 680. If this value of $R_{k,\infty} = 680$ is used as a criterion for transition, it becomes a simple matter to determine whether a given height of distributed roughness will cause transition for a given airfoil Reynolds number. If this criterion is expressed in terms of the nominal size of the roughness grain, the corresponding critical value of $R_{k,\infty}$ is 415. This criterion agrees very well with the data presented in references 7 and 8.

Although a particular pressure distribution was involved in the determination of the simple criterion $R_{k,\infty} = 680$, it seems reasonable that the critical value should not be very sensitive to the particular type of pressure distribution. In general, if it is assumed that the value of $R_{k,t}$ is 600 for the case where the height of the roughness is less than the total boundary-layer thickness and is at least as large or larger for roughness that projects through the boundary layer, this condition will correspond to a value of $R_{k,\infty}$ of about 680 if the airfoil has a reasonably extensive region of low pressure gradient with a velocity outside the boundary layer approximately equal to the free-stream velocity. Consider, for example, the case of a flat plate with uniform pressure. If the roughness is so far forward that it projects through the boundary layer, the value of $R_k$ will not change with further forward movement of the roughness. The data of figure 13 seem to indicate, however, that the value of $R_{k,t}$ has its lowest value when the roughness is just completely immersed in the boundary layer. For this case, the value of $R_{k,t}$ is 600 and the corresponding value of $R_{k,\infty}$ for a flat plate would be only slightly greater than this value and thus would not differ greatly from the value of 680 found for the present airfoil.

The minimum size of roughness that can be easily detected or the size of the splattered remains of insects are relatively fixed values completely independent of wing size. In view of these conditions, the significance of the unit Reynolds number $\left(R' = \frac{U_\infty}{\nu}\right)$ immediately becomes clear. For example, if $k$ is the height of the splattered remains of insects, then if $R'$ is so small that $R_{k,\infty}$ is less than about 680, the remains of the insects should not cause premature transition. If, for the sake of discussion, it is assumed that the height of the insect remains or the minimum size of roughness that can be easily detected is about 0.001 inch, the critical value of $R'$ will be about $8.2 \times 10^6$. This value of the unit Reynolds number $R'$ for transition is in general agreement with values considered acceptable on the basis of wind-tunnel experience in the Langley variable-density and low-turbulence pressure tunnels. In the variable-density-tunnel tests, in which $R'$ was usually

about $7 \times 10^6$, a fair amount of difficulty was experienced in maintaining the leading edge of the airfoils smooth enough to obtain consistent results for the maximum lift coefficients. In the low-turbulence-pressure tunnel, essentially no difficulty was experienced in obtaining the design laminar flow for a unit Reynolds number $R' = 1.5 \times 10^6$ and only occasional difficulties for $R' = 3 \times 10^6$; however, for $R'$ above these values, the difficulty of obtaining extensive laminar flows increased markedly.

Figure 18 translates this criterion into more easily appreciated terms. The critical size of roughness for an assumed free-stream Mach number of 1.0 has been computed as a function of altitude by using NACA standard atmosphere (ref. 15). At sea level, the critical size is about 0.001 inch. This increases to about 0.002 inch at 20,000 feet and 0.010 inch at 60,000 feet. For altitudes above 30,000 or 40,000 feet, it does not seem likely that accidental surface roughness should make it difficult to obtain extensive laminar flows. Of course, built-in roughness such as lap or butt joints, surface waviness, or rivet heads might still be sufficiently large to cause transition.

## CONCLUSIONS

A low-speed investigation in the Langley low-turbulence pressure tunnel to determine the effect of grain height and location on the transition characteristics of sandpaper type of roughness on an NACA 65-series airfoil section indicates the following conclusions:

1. If the roughness is sufficiently submerged in the boundary layer to give substantially linear variation of the boundary-layer velocity with distance from the surface up to the height of the roughness, turbulent spots begin to appear immediately behind the roughness when the Reynolds number $R_k$, based on the velocity at the top of the roughness and the roughness height, exceeds a critical value $R_{k,t}$ of approximately 600.

2. At Reynolds numbers even slightly below the critical value, the sandpaper type of roughness introduced no measurable disturbances into the laminar layer downstream of the roughness.

3. The most sensitive position for roughness grains of a given size, that is, the roughness position for which the critical value of the model Reynolds number is least, is that at which the roughness height is slightly less than the total laminar boundary-layer thickness.

4. The chordwise extent of the roughened area does not appear to have an important effect on the critical value of the roughness Reynolds number $R_{k,t}$.

5. If the airfoil has a reasonably extensive region of low pressure gradient with a velocity outside the boundary layer approximately equal to the free-stream velocity and roughness so distributed over the leading-edge region as to include the most sensitive position, the condition $R_{k,t} = 600$ may be approximately replaced by the more easily calculated condition $R_{k,\infty} = 680$, where $R_{k,\infty}$ is the Reynolds number based on the size of the roughness and the free-stream velocity.

Langley Aeronautical Laboratory,
National Advisory Committee for Aeronautics,
Langley Field, Va., August 15, 1956.

## REFERENCES


1. Loftin, Laurence K., Jr.: Effects of Specific Types of Surface Roughness on Boundary-Layer Transition. NACA WR L-46, 1946 (Formerly NACA ACR L5J29a.)

2. Schiller, L.: Strömung in Rohren. Handbuch der Experimentalphysik, Bd. IV, 4.Teil, Hydro- und Aerodynamik; Ludwig Schiller, Hrsg.; Akad. Verlagsgellschaft m.b.H. (Leipzig), 1932, p. 191.

3. Tani, Itiro, Hama, Ryosuke, and Mituisi, Satosi: On the Permissible Roughness in the Laminar Boundary Layer. Rep. No. 199 (vol. XV, 13), Aero. Res. Inst., Tokyo Imperial Univ., Oct. 1940.

4. Schwartzberg, Milton A., and Braslow, Albert L.: Experimental Study of the Effects of Finite Surface Disturbances and Angle of Attack on the Laminar Boundary Layer of an NACA 64A010 Airfoil with Area Suction. NACA TN 2796, 1952.

5. Klebanoff, P. S., Schubauer, G. B., and Tidstrom, K. D.: Measurements of the Effect of Two-Dimensional and Three-Dimensional Roughness Elements on Boundary-Layer Transition. Jour. Aero. Sci., vol. 22, no. 11, Nov. 1955, pp. 803-804.

6. Dryden, Hugh L.: Review of Published Data on The Effect of Roughness on Transition From Laminar to Turbulent Flow. Jour. Aero. Sci., vol. 20, no. 7, July 1953, pp. 477-482.

7. Quinn, John H., Jr.: Effects of Reynolds Number and Leading-Edge Roughness on Lift and Drag Characteristics of the NACA $65_3$-418, a = 1.0 Airfoil Section. NACA WR L-82, 1945. (Formerly NACA CB L5J04.)

8. Loftin, Laurence K., Jr. and Smith, Hamilton A.: Aerodynamic Characteristics of 15 NACA Airfoil Sections at Seven Reynolds Numbers From $0.7 \times 10^6$ to $9.0 \times 10^6$. NACA TN 1945, 1949.

9. Braslow, Albert L., and Visconti, Fioravante: Investigation of Boundary-Layer Reynolds Number for Transition on an NACA $65_{(215)}$-114 Airfoil in the Langley Two-Dimensional Low-Turbulence Pressure Tunnel. NACA TN 1704, 1948.

10. Von Doenhoff, Albert E., and Abbott, Frank T., Jr.: The Langley Two-Dimensional Low-Turbulence Pressure Tunnel. NACA TN 1283, 1947.

11. Quinn, John H., Jr.: Drag Tests of an NACA $65_{(215)}$-114, a = 1.0 Practical-Construction Airfoil Section Equipped with a 0.295-Airfoil-Chord Slotted Flap. NACA TN 1236, 1947.

12. Anon: Abrasive Grain Sizes. Simplified Practice Recommendation 118-50, U. S. Dept. Commerce, June 1, 1950.

13. Schlichting, Hermann (J. Kestin, trans.): Boundary Layer Theory. McGraw-Hill Book Co., Inc., 1955, ch. 12, pt. B.

14. Schubauer, G. B. and Klebanoff, P. S.: Contributions on the Mechanics of Boundary-Layer Transition. NACA TN 3489, 1955.

15. Anon: Standard Atmosphere - Tables and Data for Altitudes to 65,800 feet. NACA Rep. 1235, 1955. (Formerly NACA TN 3182.)

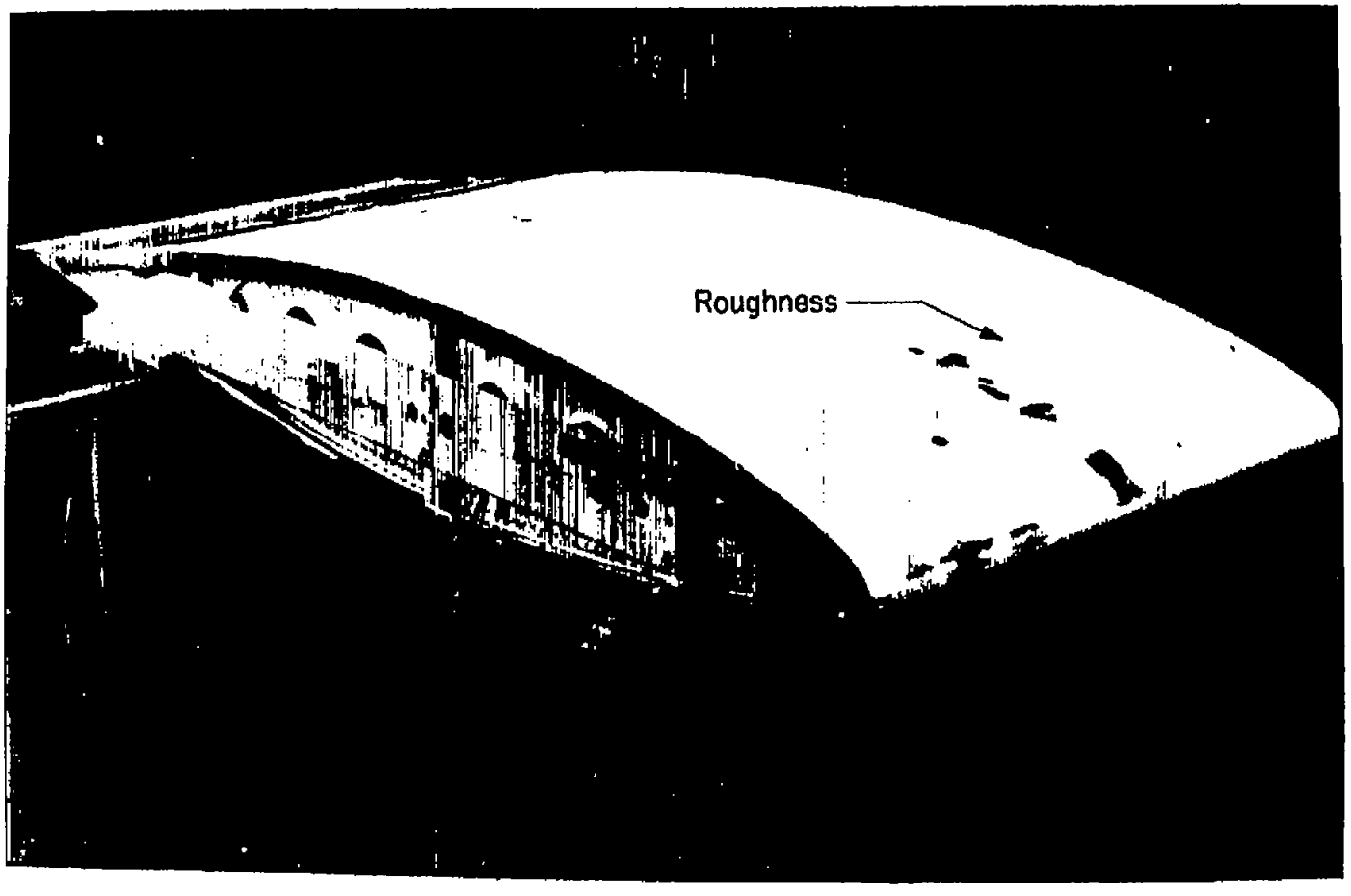


L-90417.1

Figure 1.- Three-quarter view of 85-inch-chord NACA $65_{(215)}$-114 airfoil section with No. 60 carborundum grains from forward stagnation point to 12-inch station.

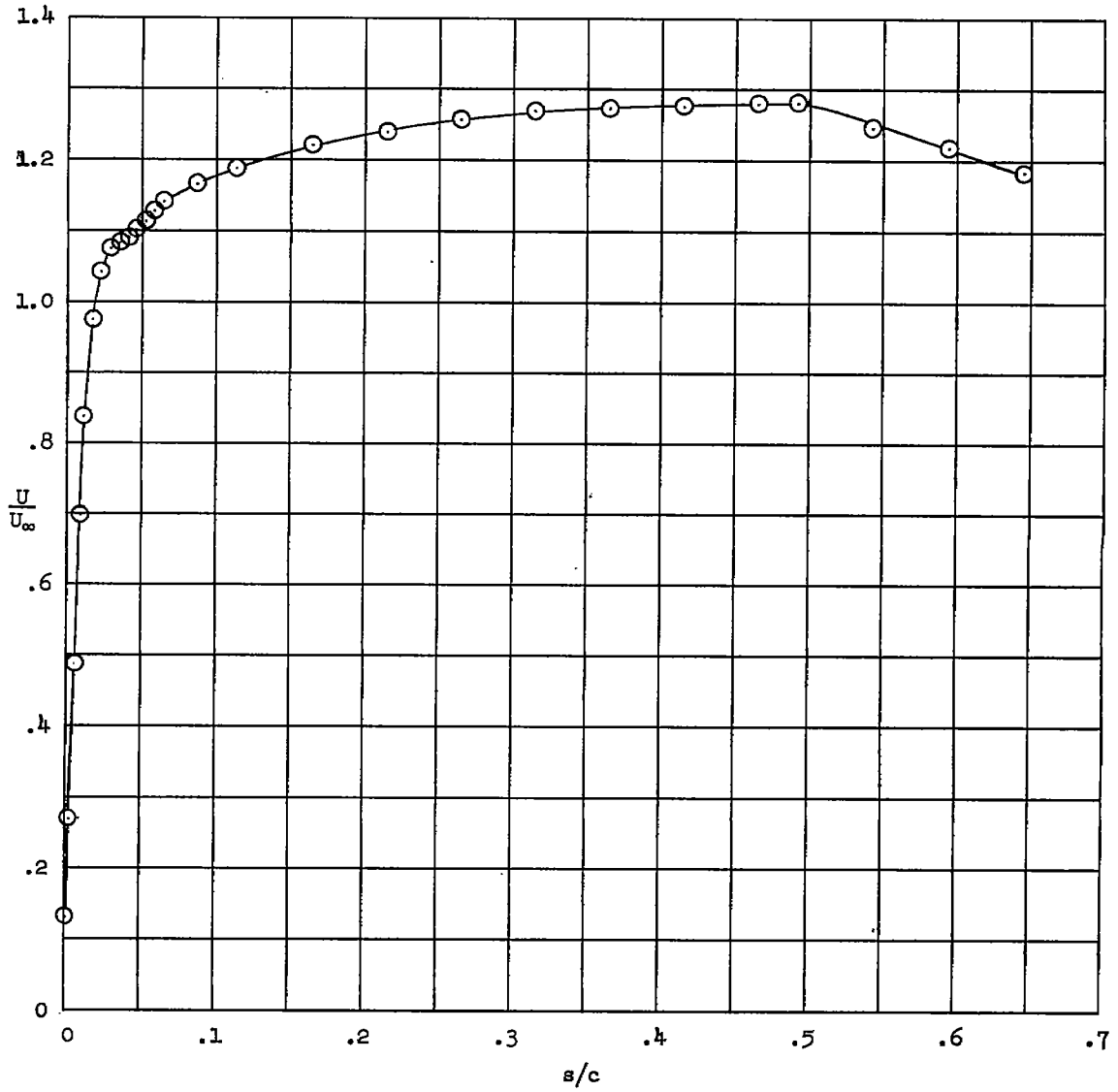


Figure 2.- Nondimensional velocity distribution outside of the boundary layer for NACA $65_{(215)}$-114 airfoil section at angle of attack of $0^\circ$.

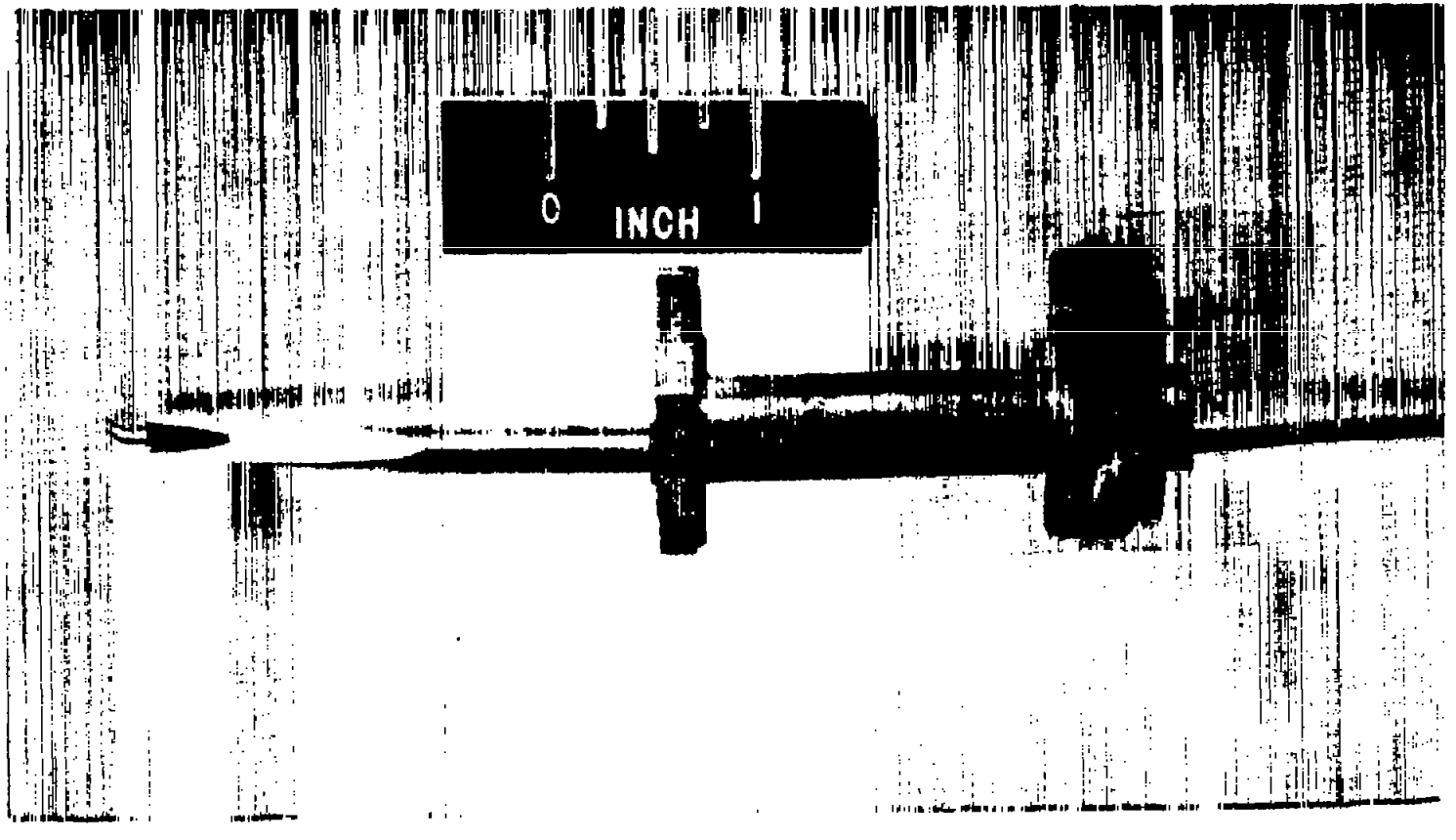


L-90896

Figure 3.- Hot-wire holder used in investigation.

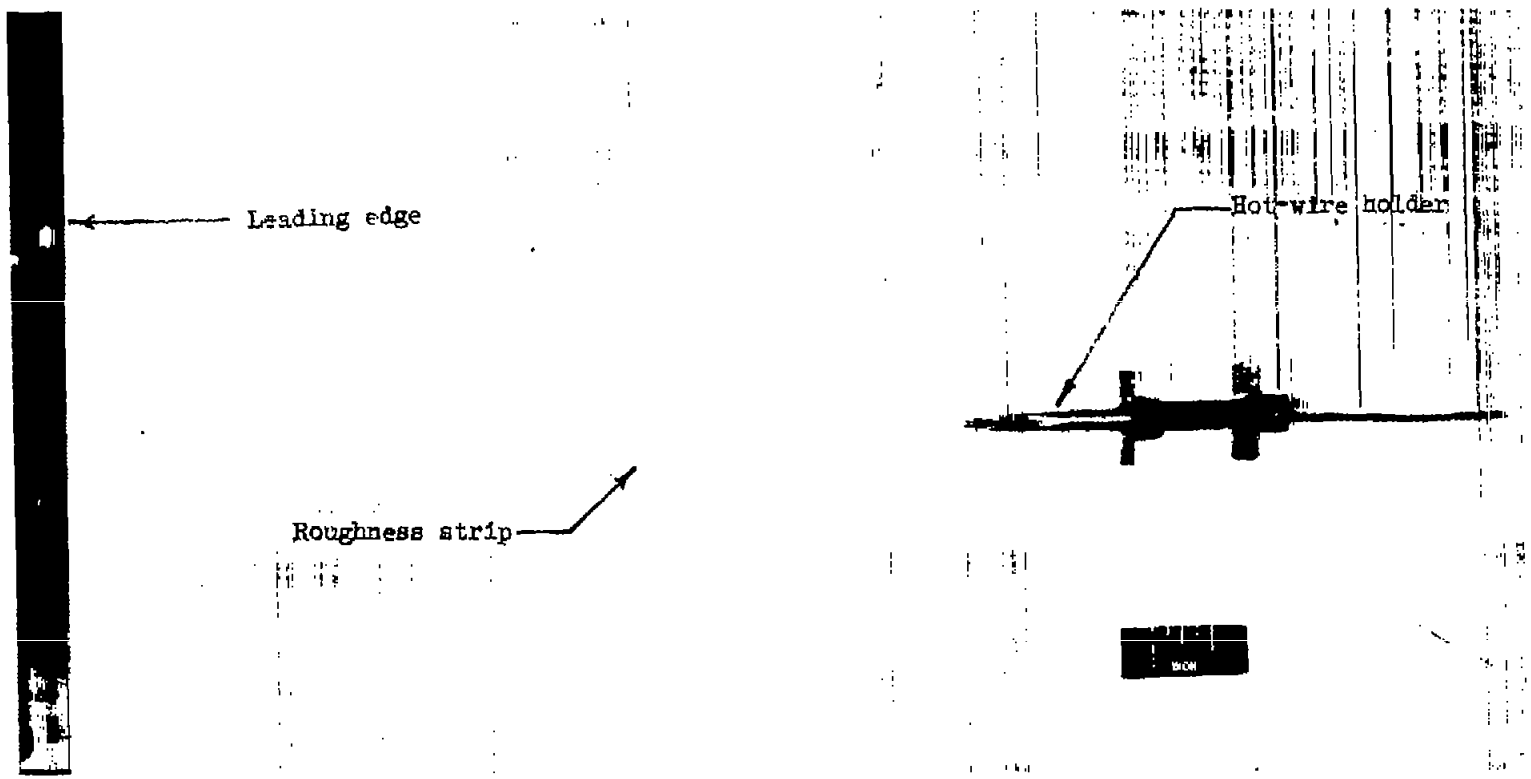


L-90895.1

Figure 4.- View of hot-wire holder mounted on the airfoil surface relative to a typical $\frac{1}{4}$-inch by 1-inch roughness strip.

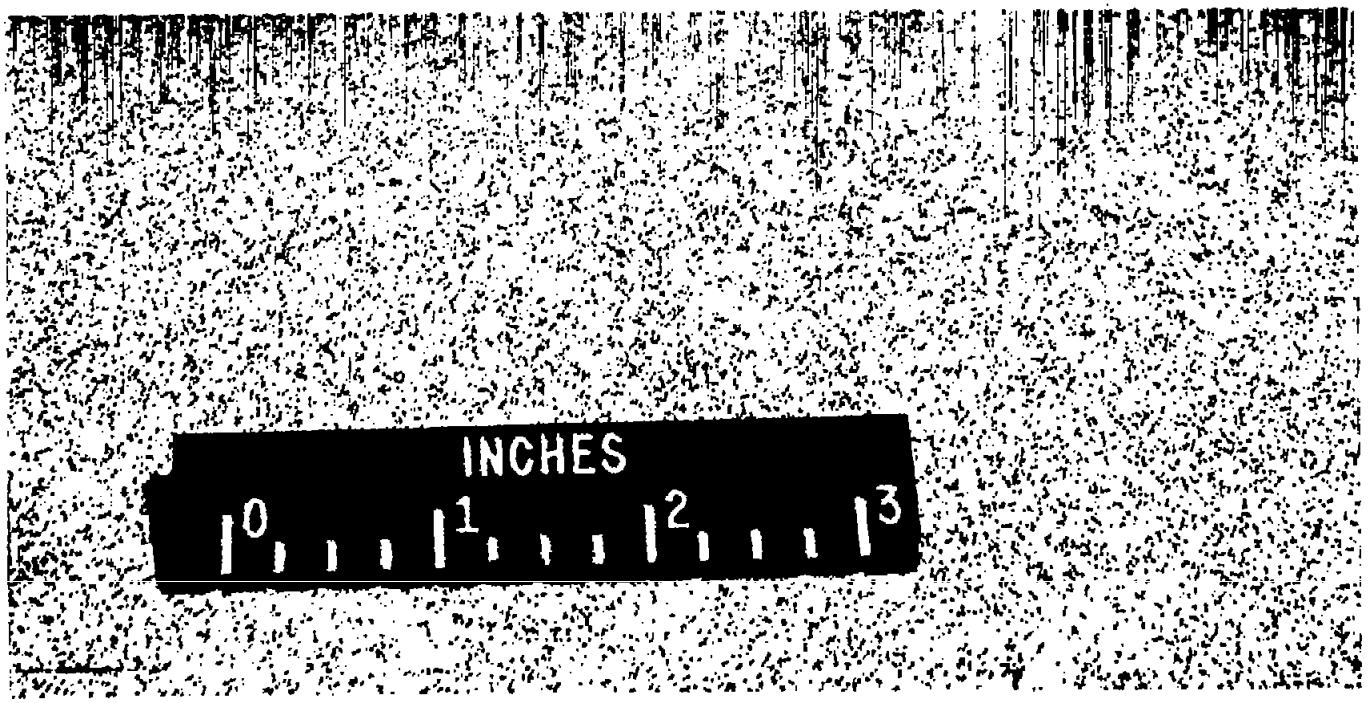


Figure 5.- Closeup of distributed No. 60 carborundum grains. L-90418.1

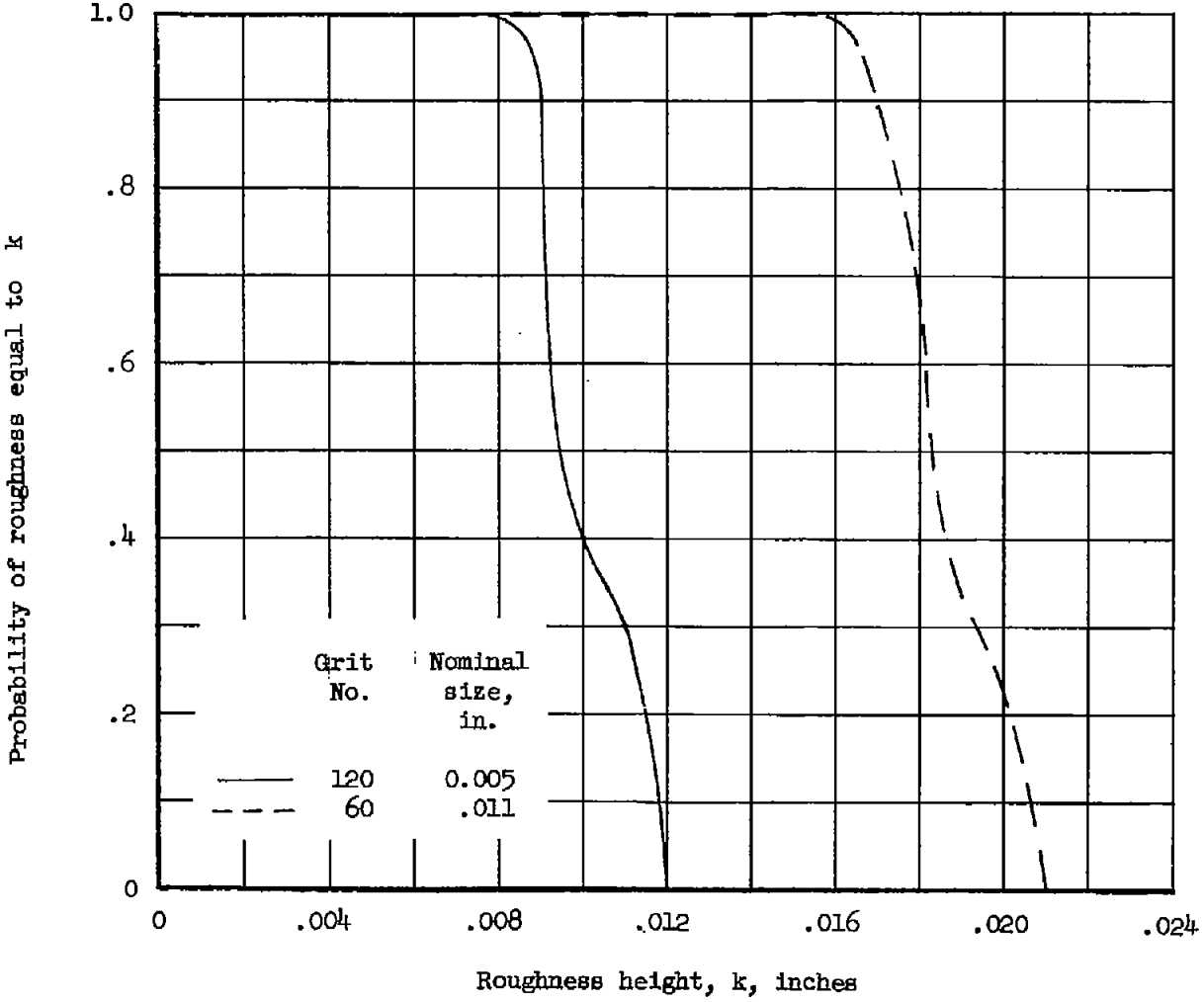


Figure 6.- Curves showing the probability of finding at least one grain of a given size of roughness in any 1/4-inch by 1-inch roughness area when nominal size of carborundum grains is 0.005 or 0.011 inch.

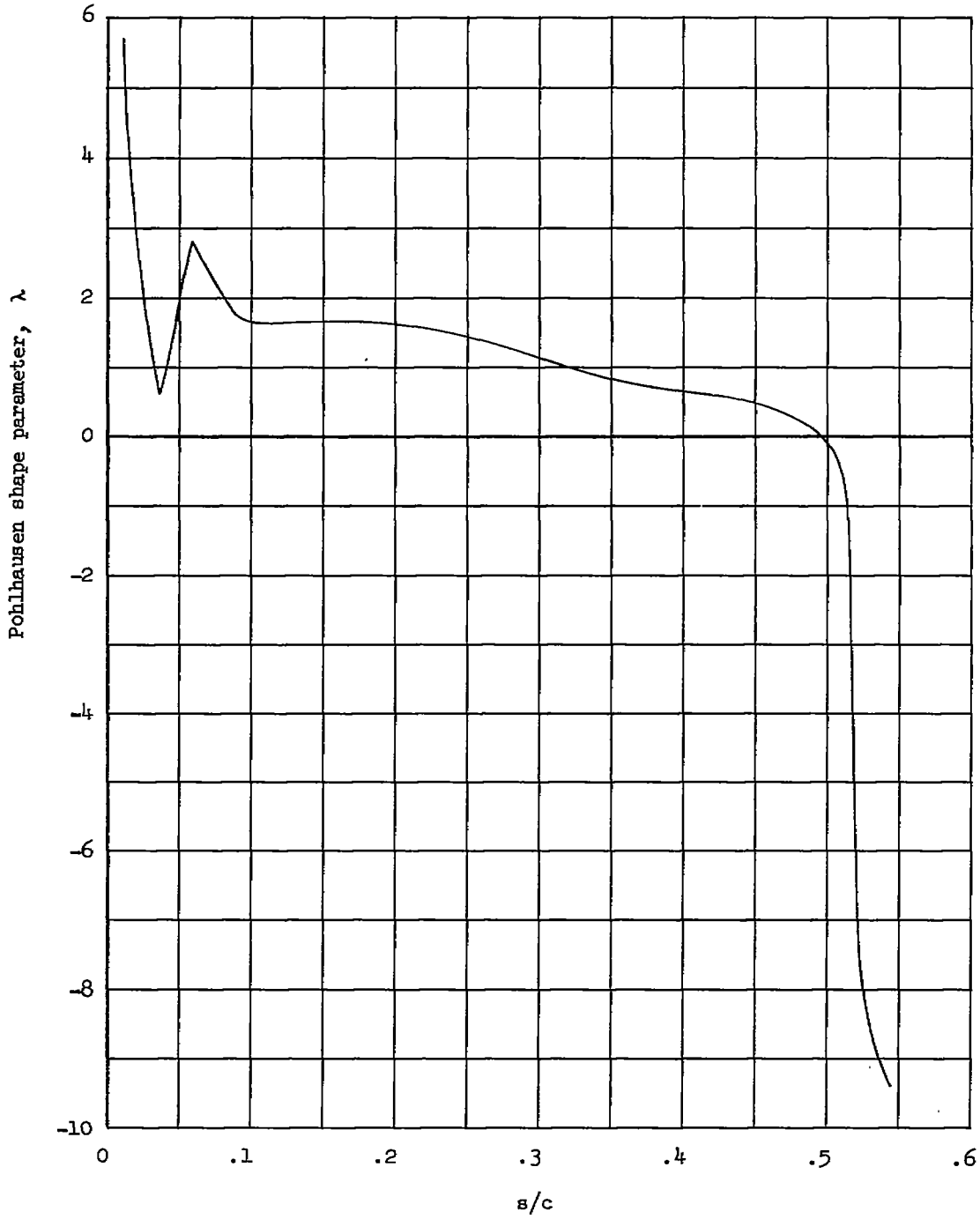


Figure 7.- Pohlhausen shape parameter $\lambda$ for a laminar boundary layer on NACA $65_{(215)}$-114 airfoil section at angle of attack of $0^{\circ}$.

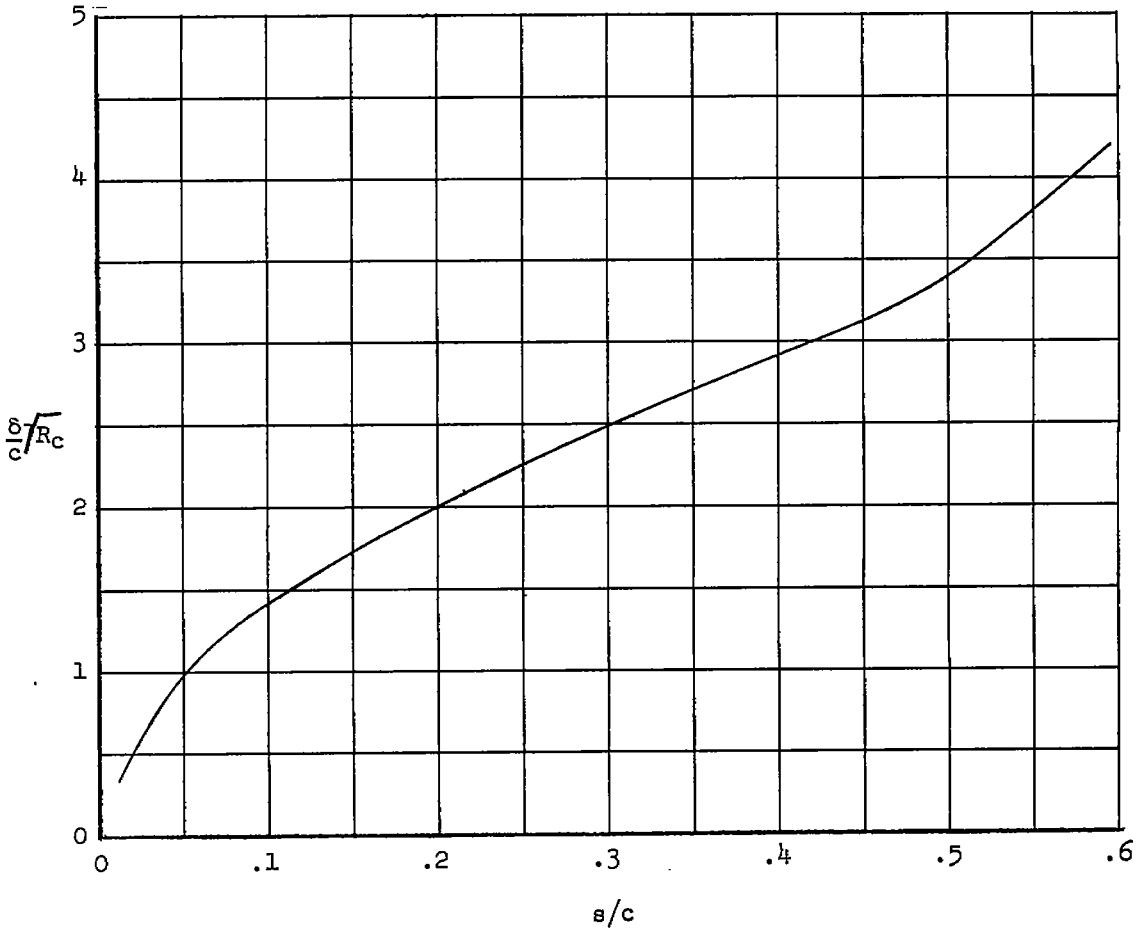


Figure 8.- Nondimensional laminar-boundary-layer thickness distribution for NACA 65(215)-114 airfoil section.

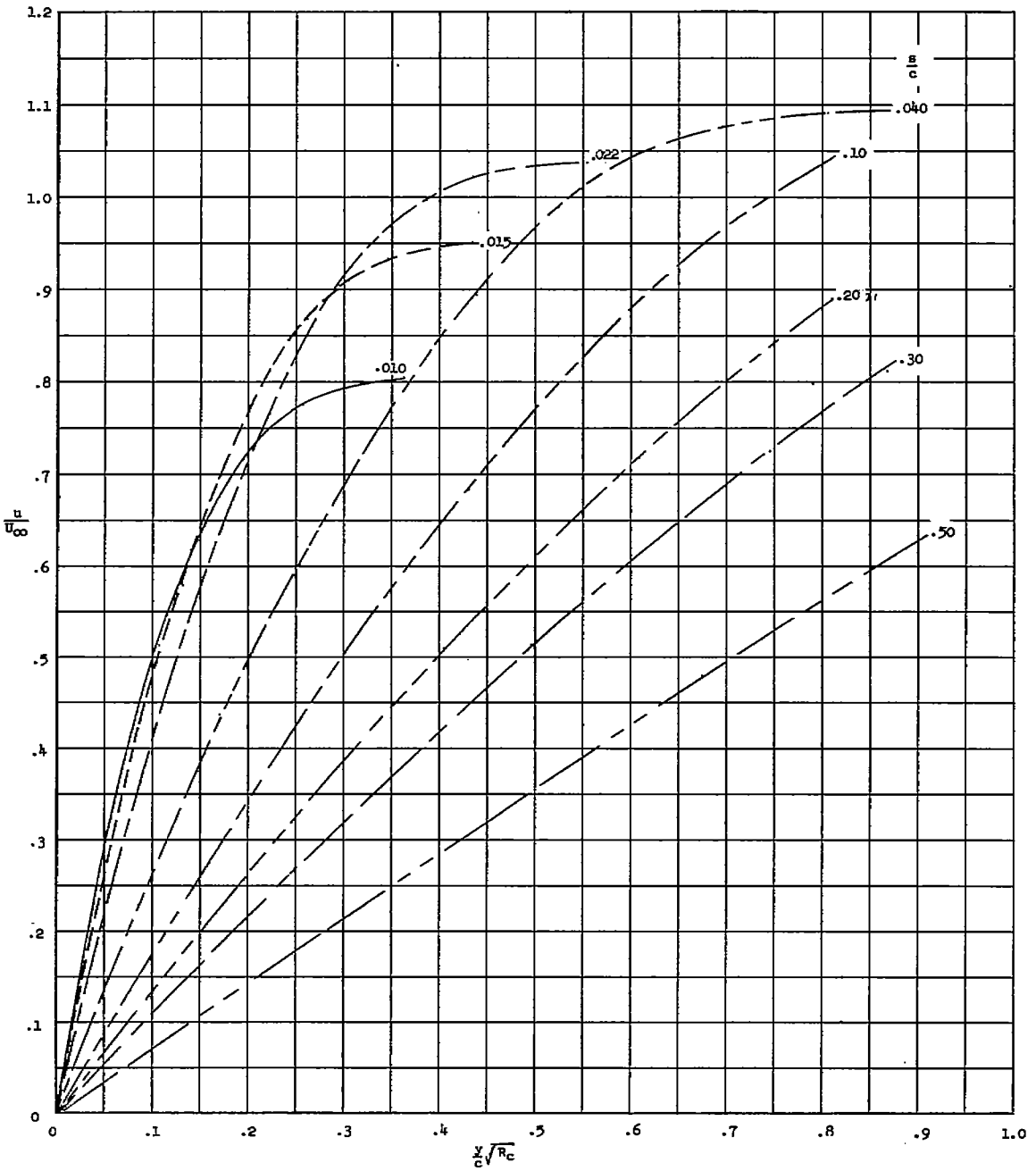


Figure 9.- Nondimensional velocity distribution within laminar boundary layer of NACA 65(215)-114 airfoil section for various positions along surface.

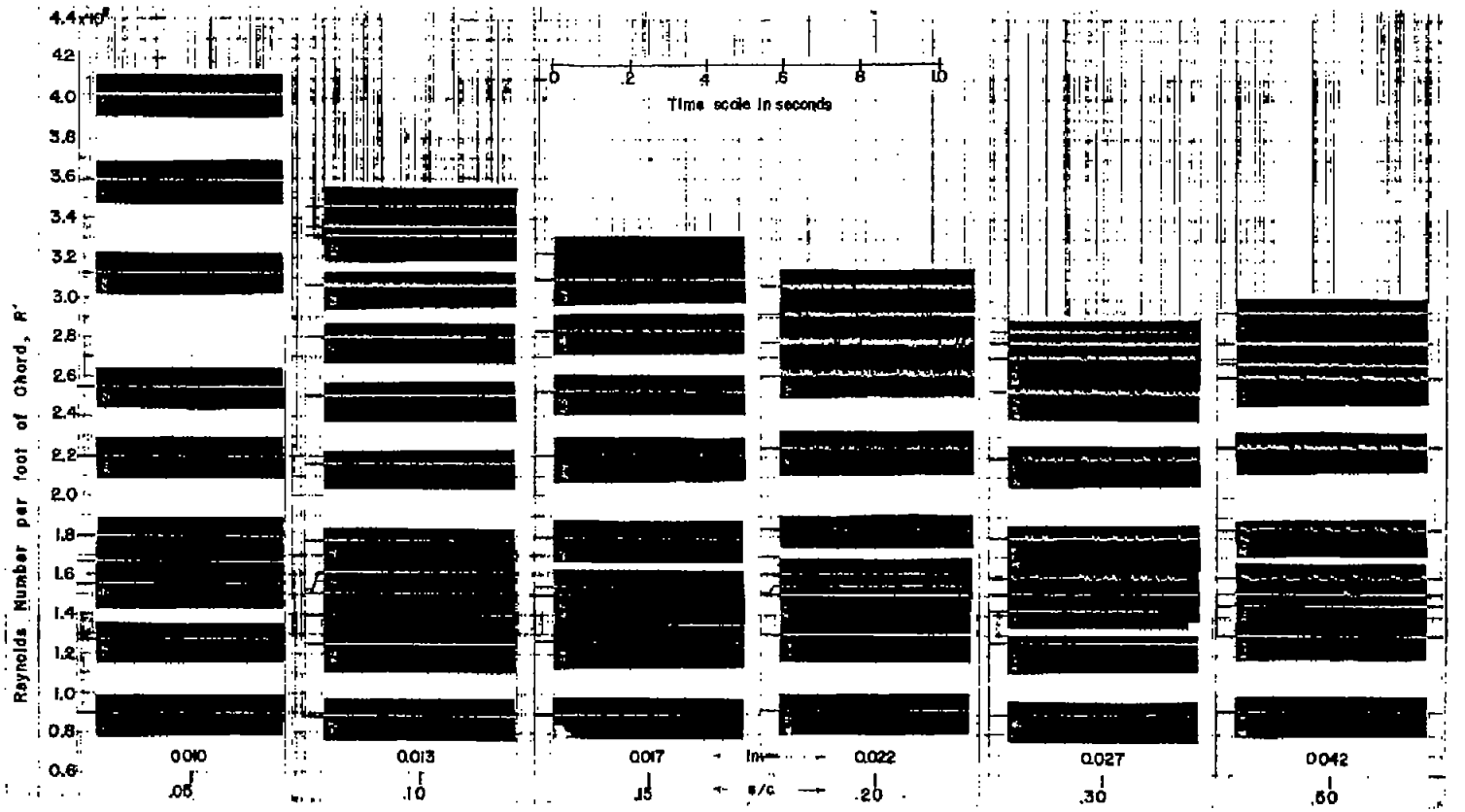


Hot-wire location back of forward stagnation point and distance above surface

(a) No. 60 carborundum from 0.25 to 0.50 inch back of forward stagnation point.

Figure 10.- Typical oscillograph records at various chordwise positions through transition-speed range for 85-inch-chord NACA 65(215)-114 airfoil section with various locations and sizes of roughness.

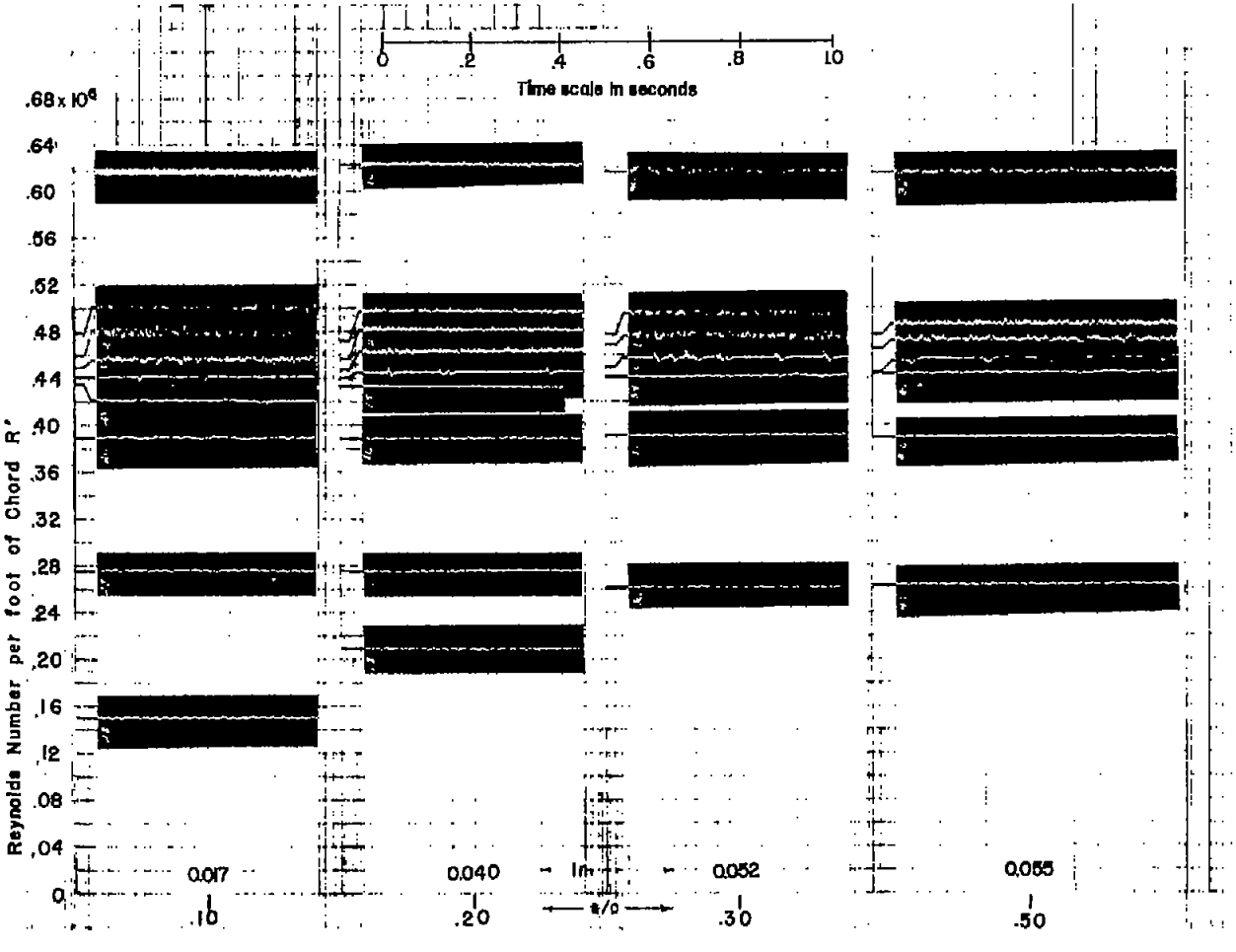


Hot-wire location back of forward stagnation point and distance above surface

(b) No. 60 carborundum from 2.0 to 2.25 inches back of forward stagnation point.

Figure 10.- Continued.

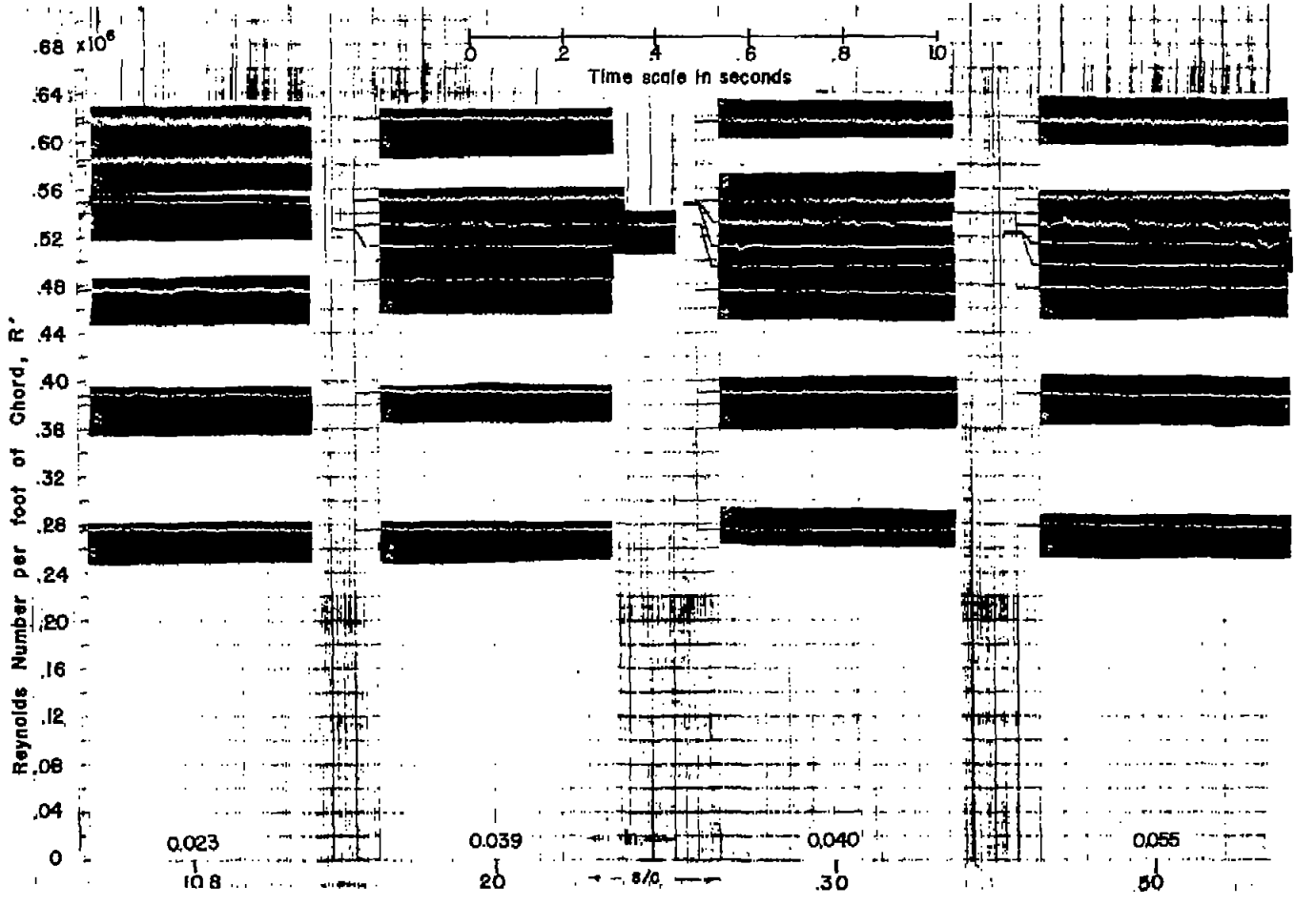


Hot-wire location back of forward stagnation point and distance above surface

(c) No. 60 carborundum from 6.5 to 6.75 inches back of forward stagnation point.

Figure 10.- Continued.

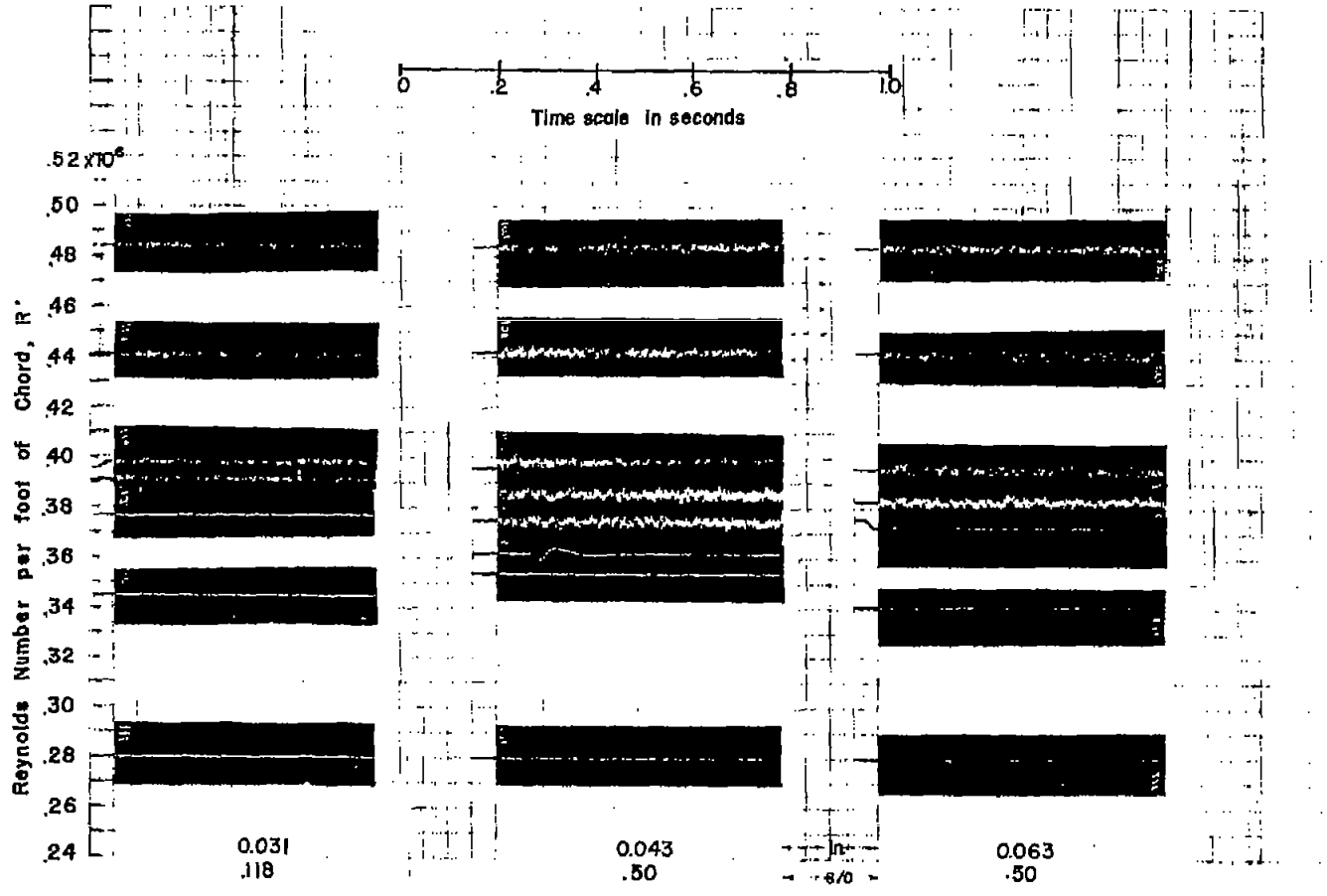


Hot-wire location back of forward stagnation point and distance above surface

(d) No. 60 carborundum from 0 to 6 inches back of forward stagnation point.

(e) No. 60 carborundum from 0 to 12 inches back of forward stagnation point.

Figure 10.- Continued.

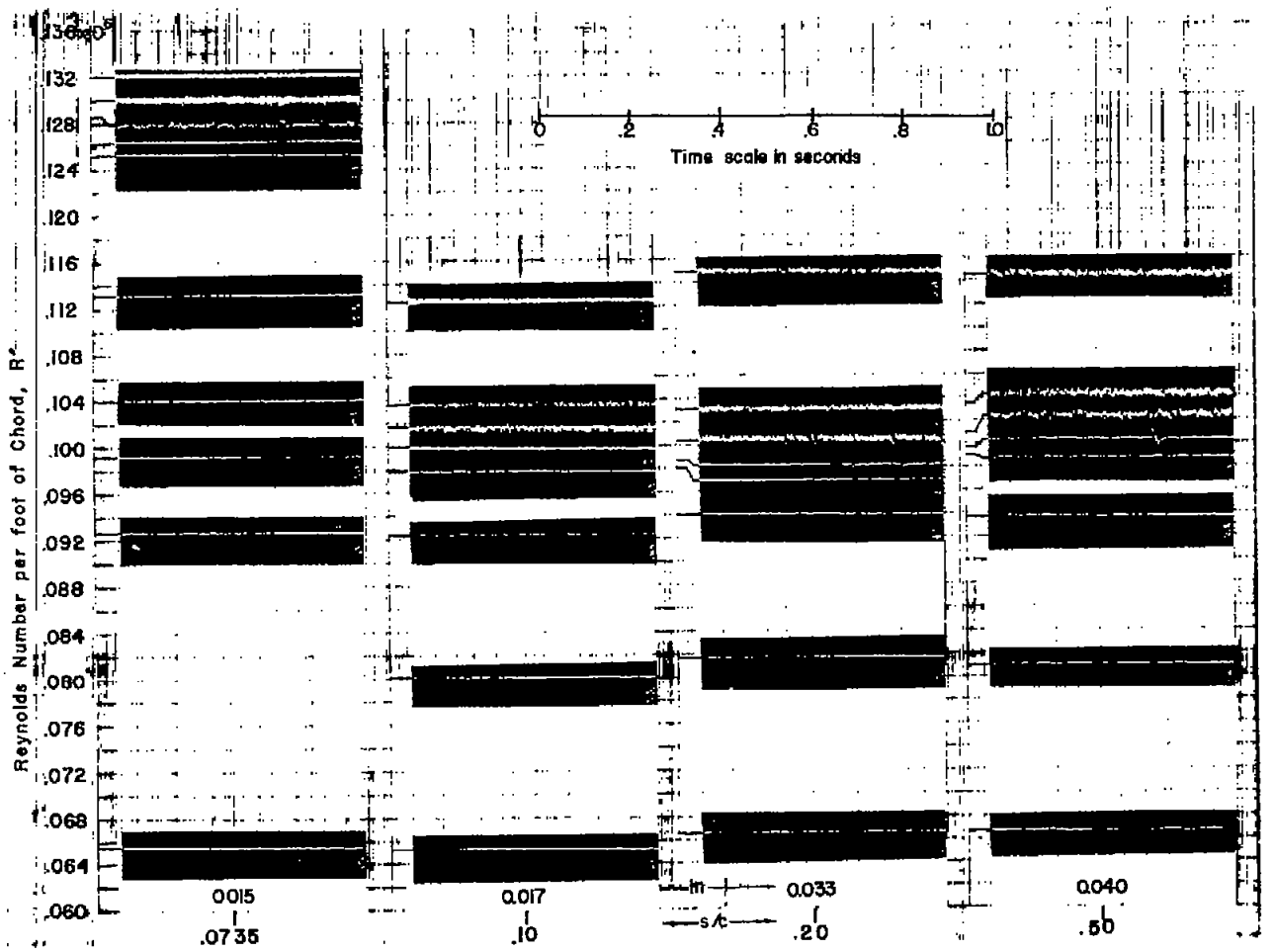


Hot-wire location back of forward stagnation point and distance above surface

(f) No. 120 carborundum from 2.00 to 2.25 inches back of forward stagnation point.

Figure 10.- Concluded.

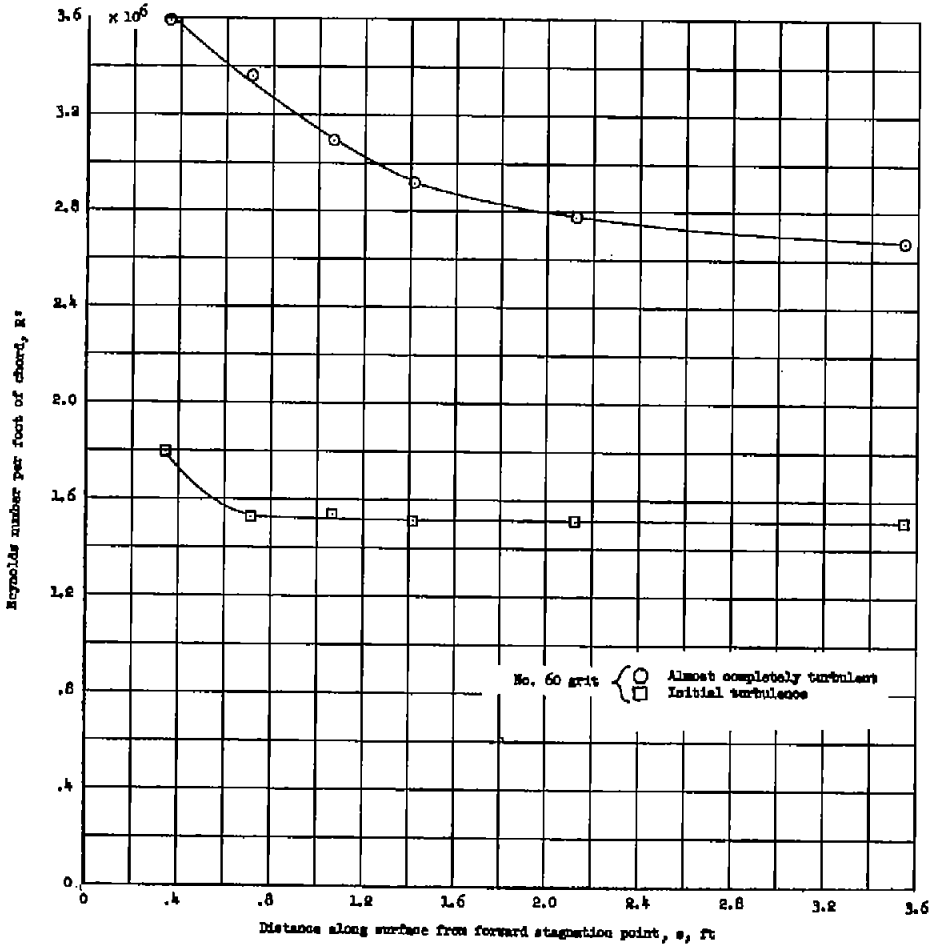


(a) Roughness located from 0.25 to 0.50 inch from forward stagnation point.

Figure 11.- Reynolds number per foot at which transition occurs at various chordwise positions for an NACA 65(215)-114 airfoil section with No. 60 and No. 120 carborundum at various chordwise positions.

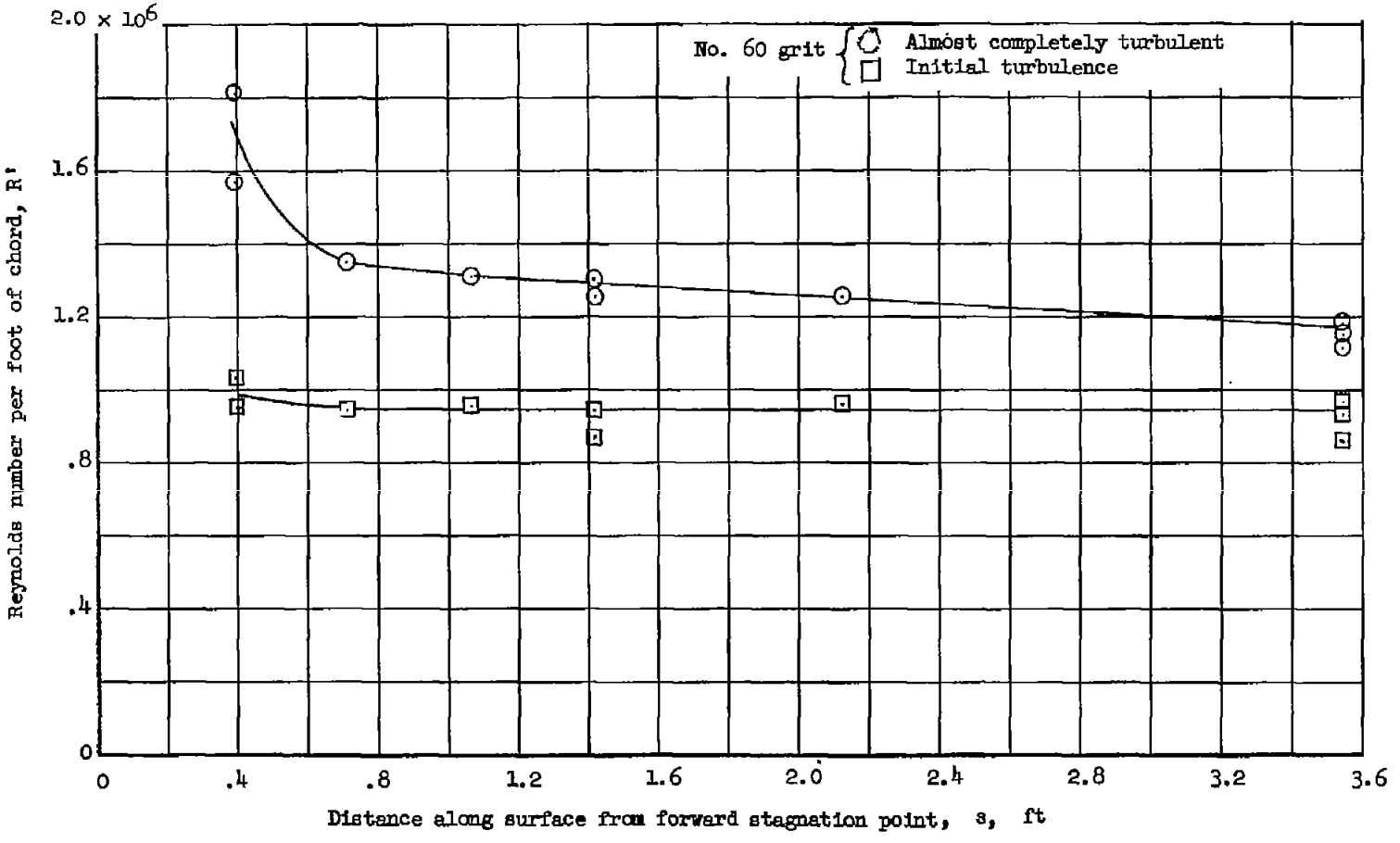


(b) Roughness located from 0.50 to 0.75 inch from forward stagnation point.

Figure 11.- Continued.

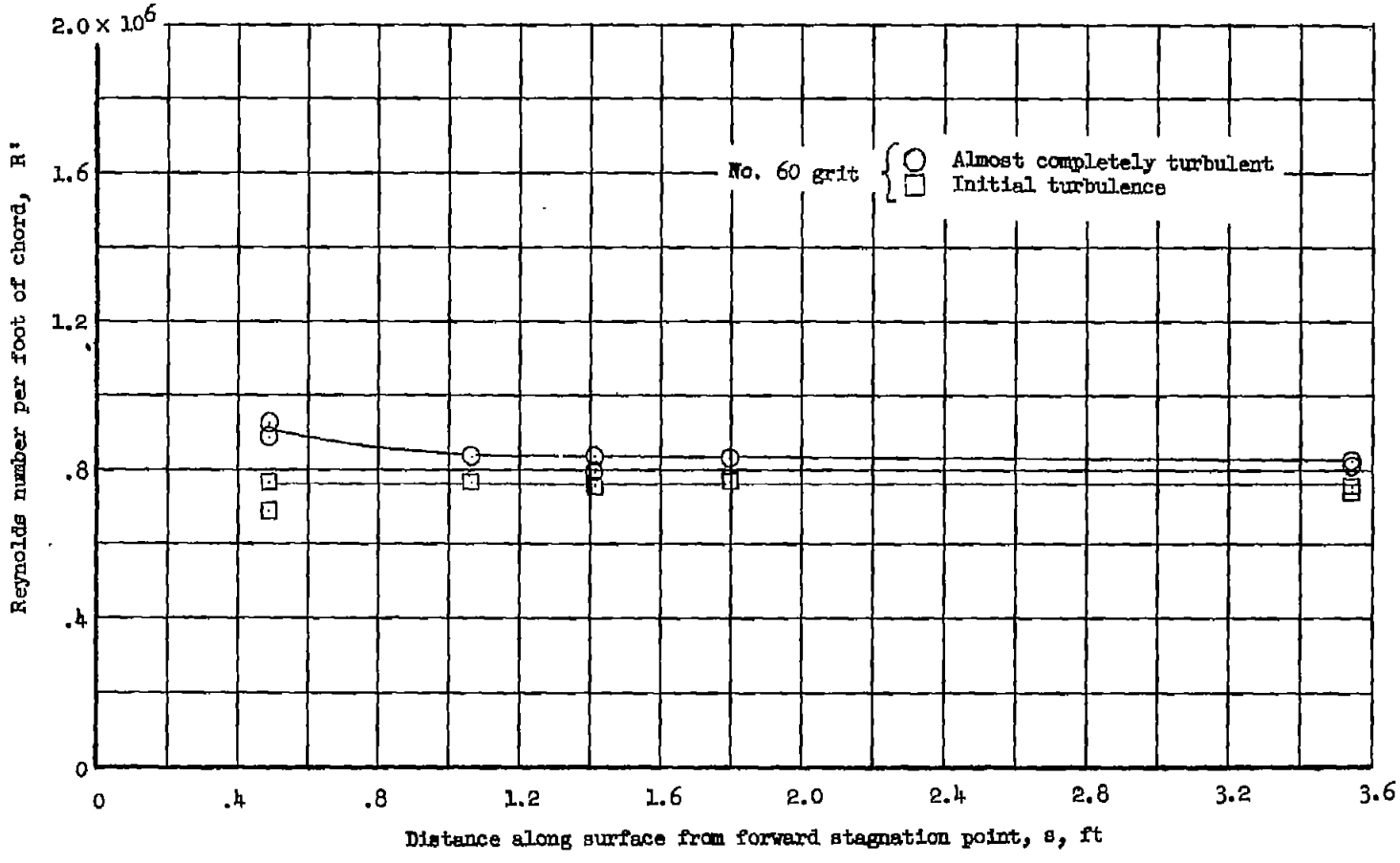


(c) Roughness located from 0.75 to 1.00 inch from forward stagnation point.

Figure 11.- Continued.

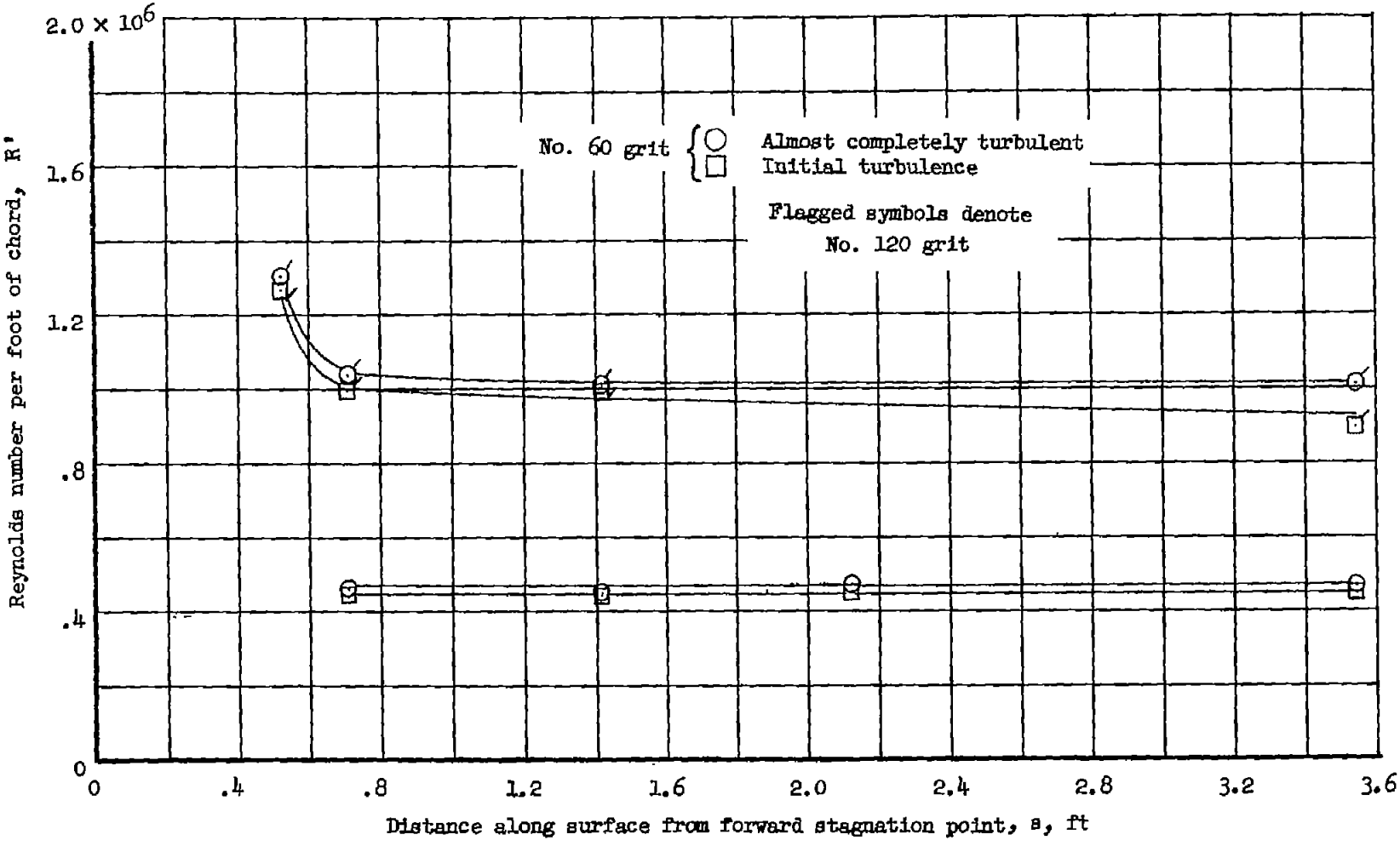


(d) Roughness located from 2.00 to 2.25 inches from forward stagnation point.

Figure 11.- Continued.

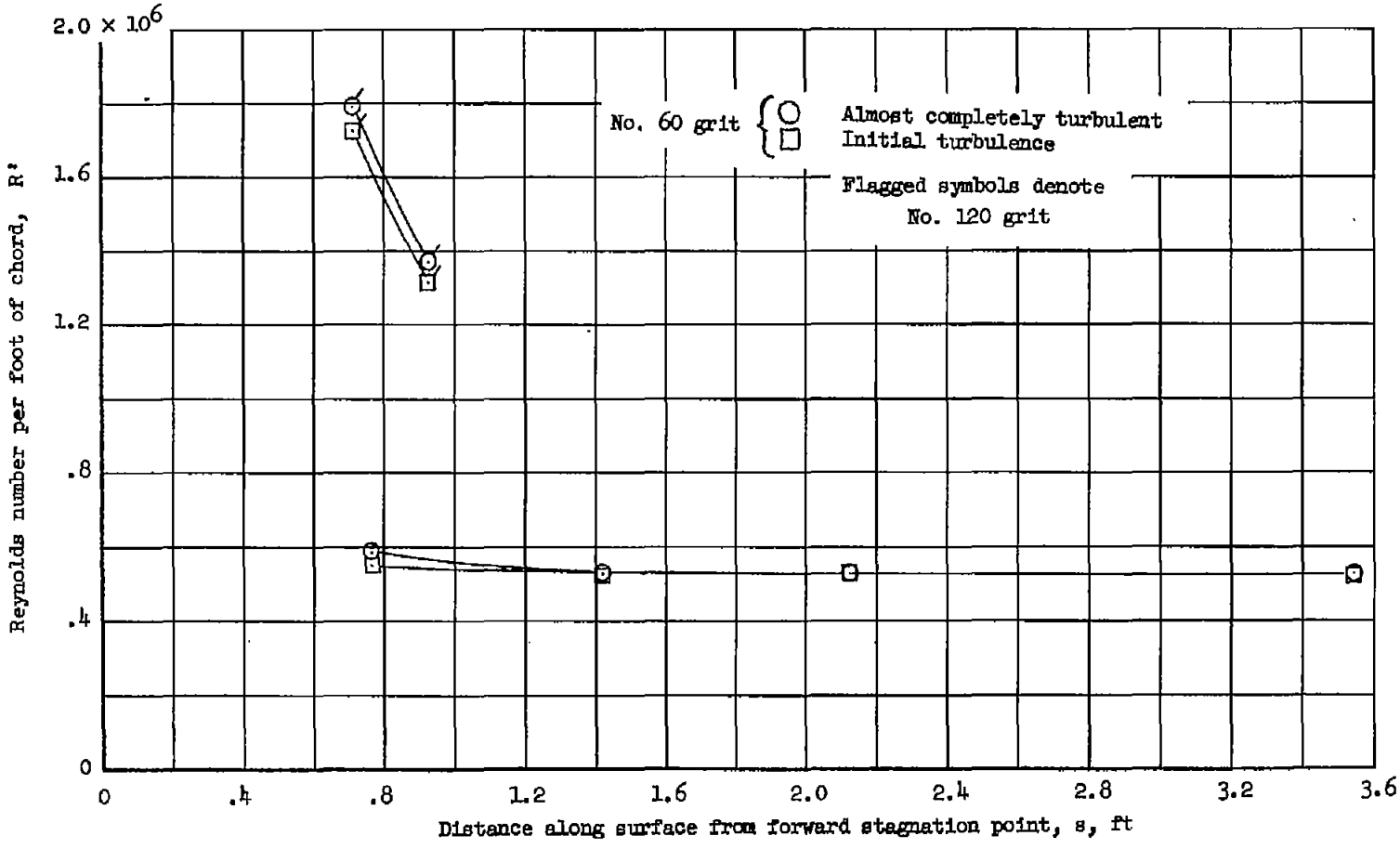


(e) Roughness located from 6.5 to 6.75 inches from forward stagnation point.

Figure 11.- Continued.

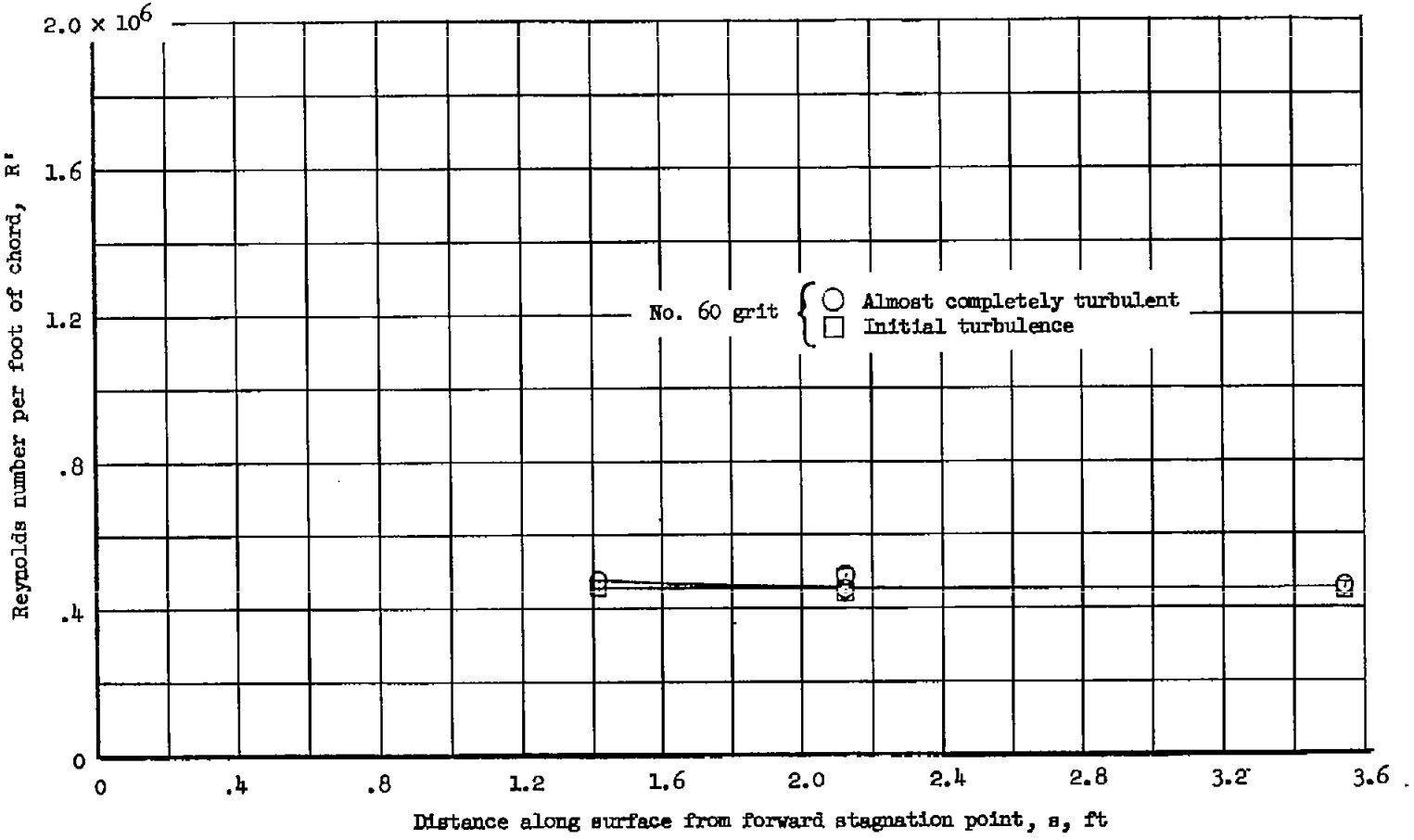


(f) Roughness located from 12.00 to 12.25 inches from forward stagnation point.

Figure 11.- Concluded.

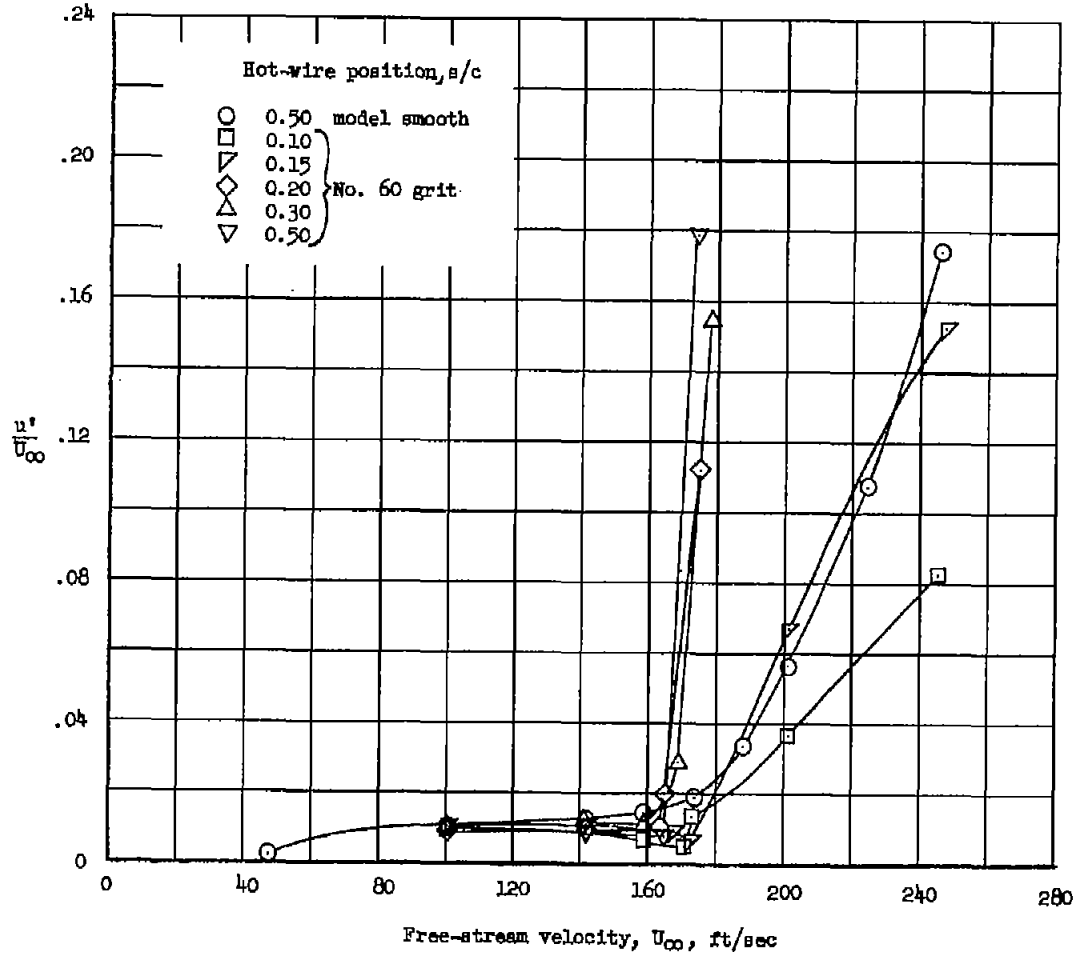


(a) Roughness from 0.25 to 0.50 inch back of forward stagnation point.

Figure 12.- Turbulence-level measurements $u'/U_\infty$ on NACA 65(215)-114 airfoil section as a function of free-stream velocity $U_\infty$ for model smooth and three representative locations of the roughness.

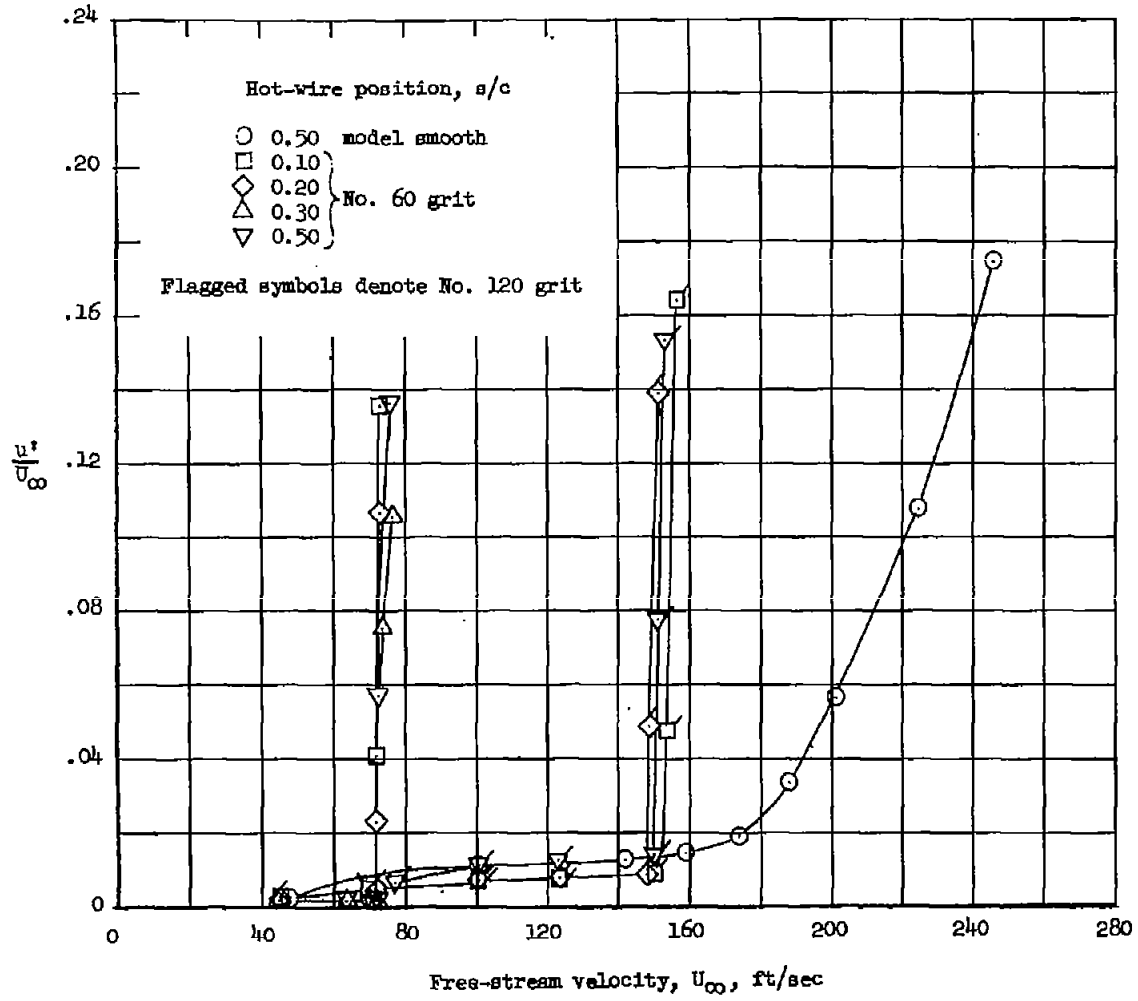


(b) Roughness from 2.00 to 2.25 inches back of forward stagnation point.

Figure 12.- Continued.

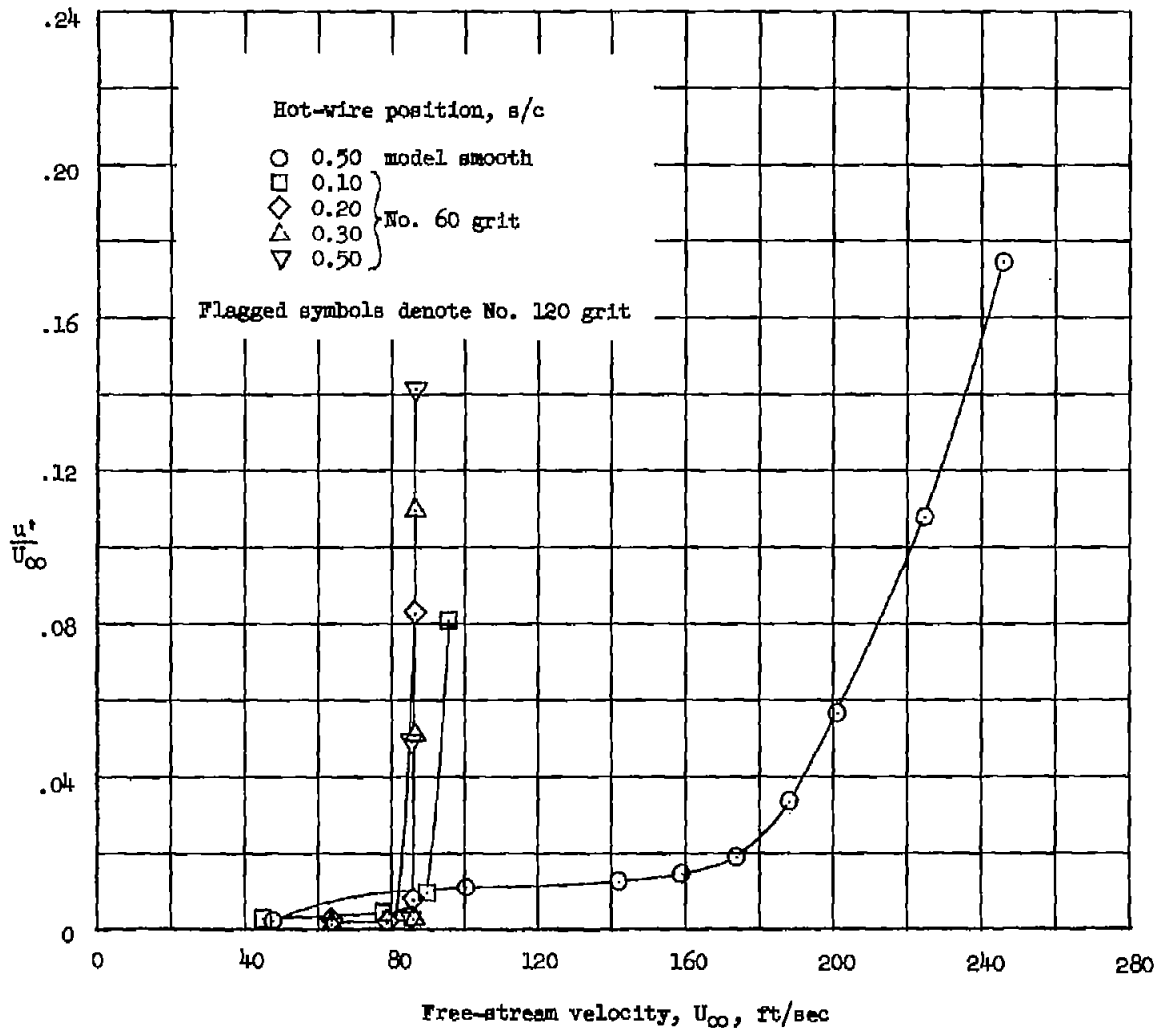


(c) Roughness from 6.50 to 6.75 inches back of forward stagnation point.

Figure 12.- Concluded.

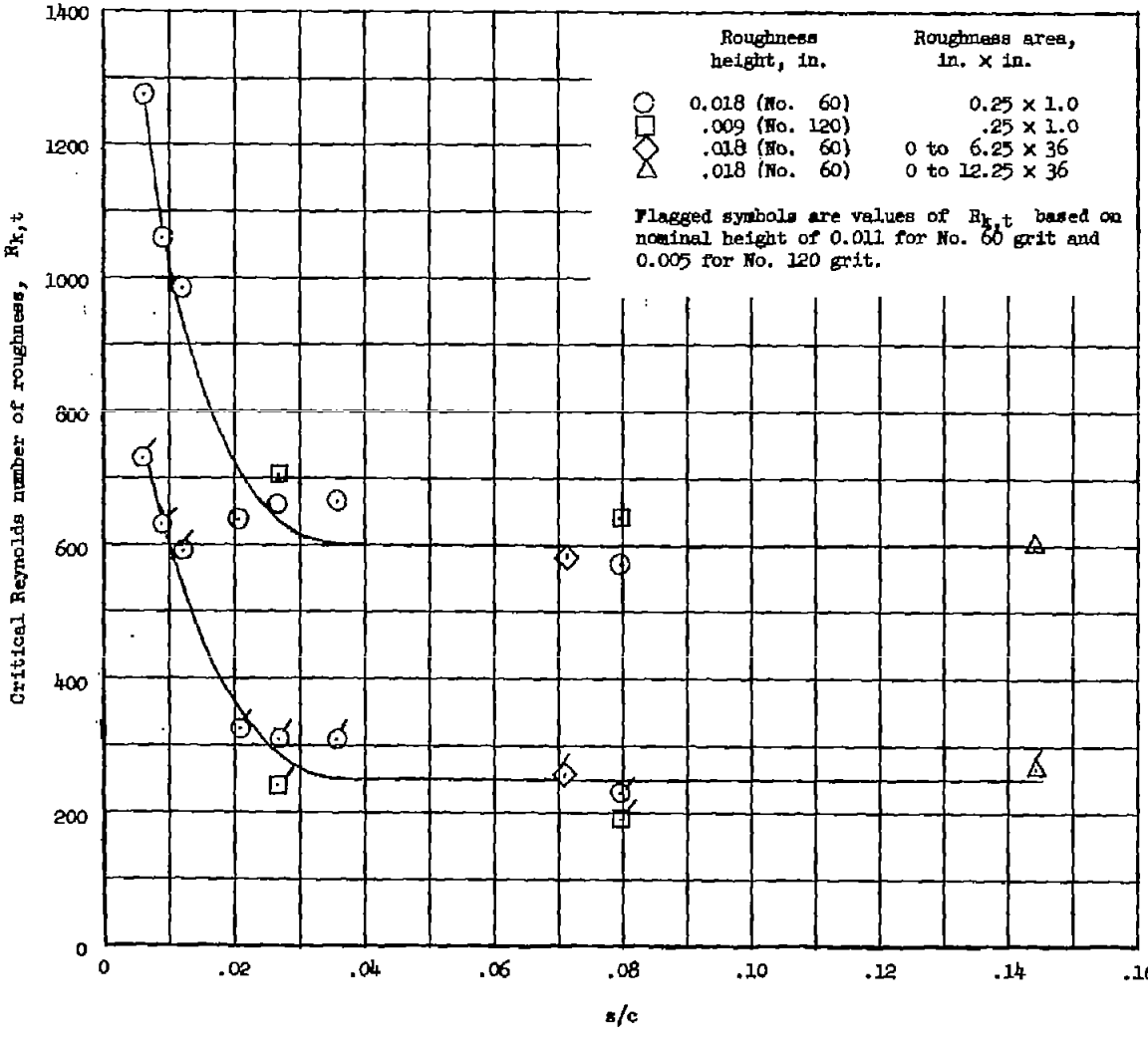


Figure 13.- Roughness Reynolds number for transition on NACA 65(215)-114 airfoil section as a function of roughness location.

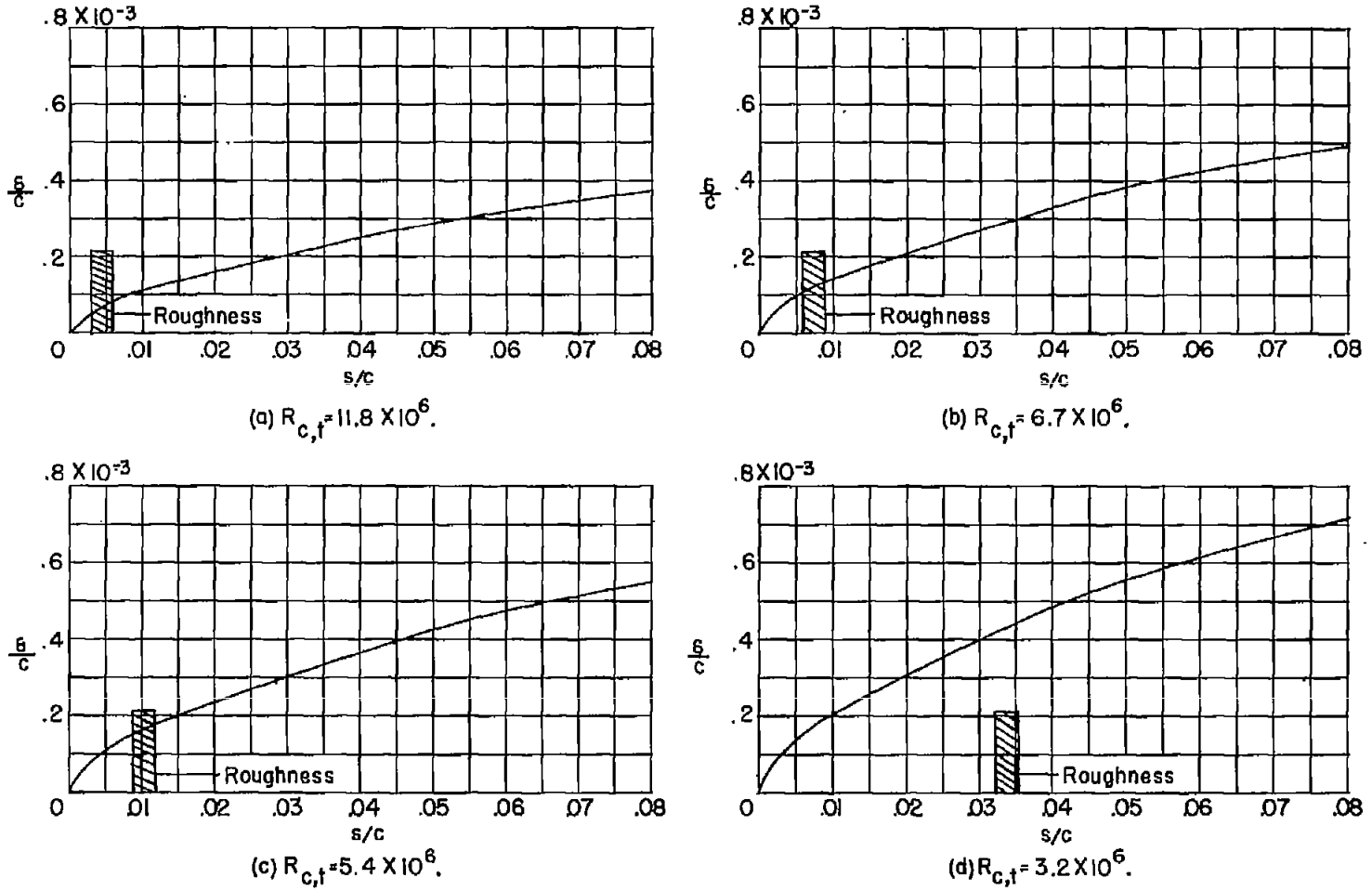


Figure 14.- Illustration of height of roughness relative to laminar-boundary-layer thickness for airfoil Reynolds number at which transition occurs for various positions of the roughness.

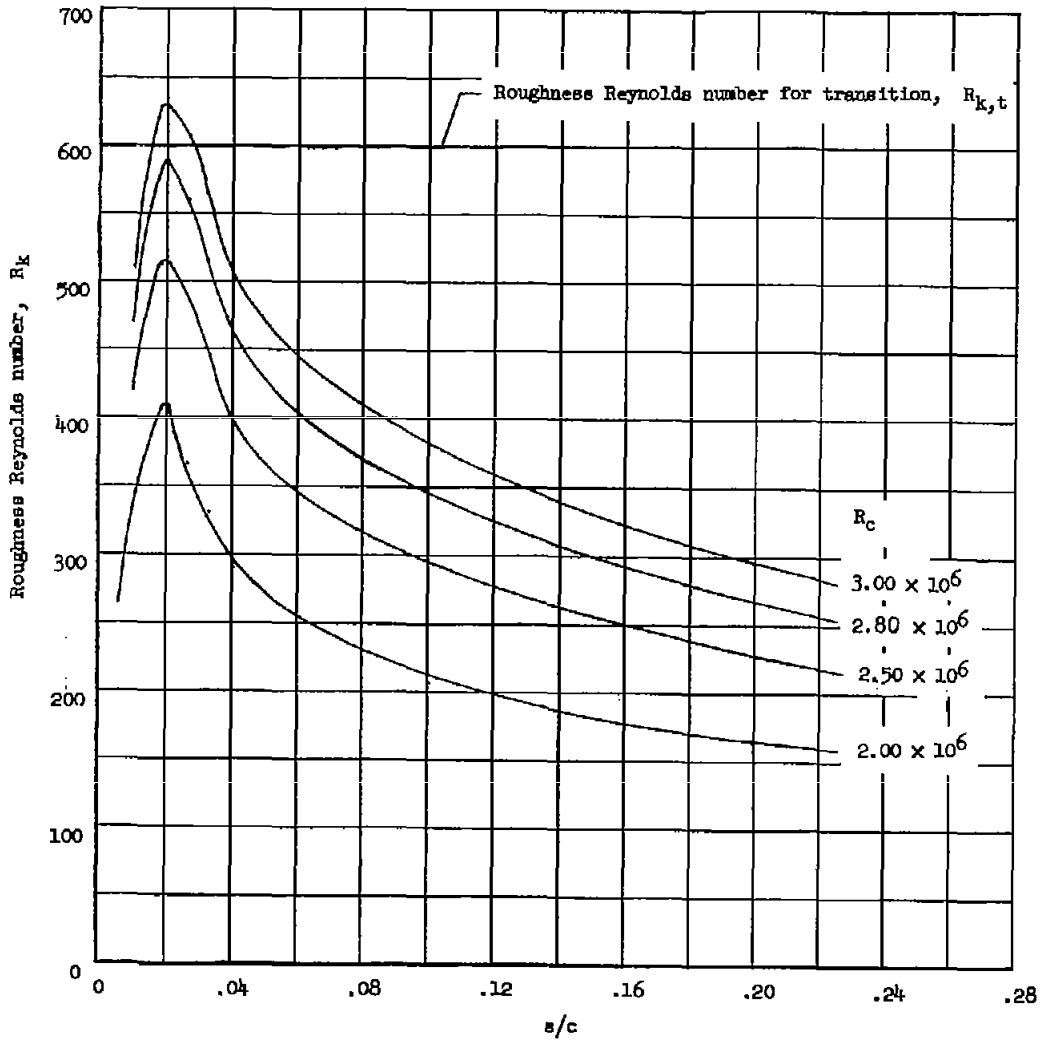


Figure 15.- The roughness Reynolds number $R_k$ for roughness height of 0.018 inch as a function of roughness location for various airfoil Reynolds numbers $R_c$ as calculated for an 85-inch-chord NACA $65_{(215)}$-114 airfoil section.

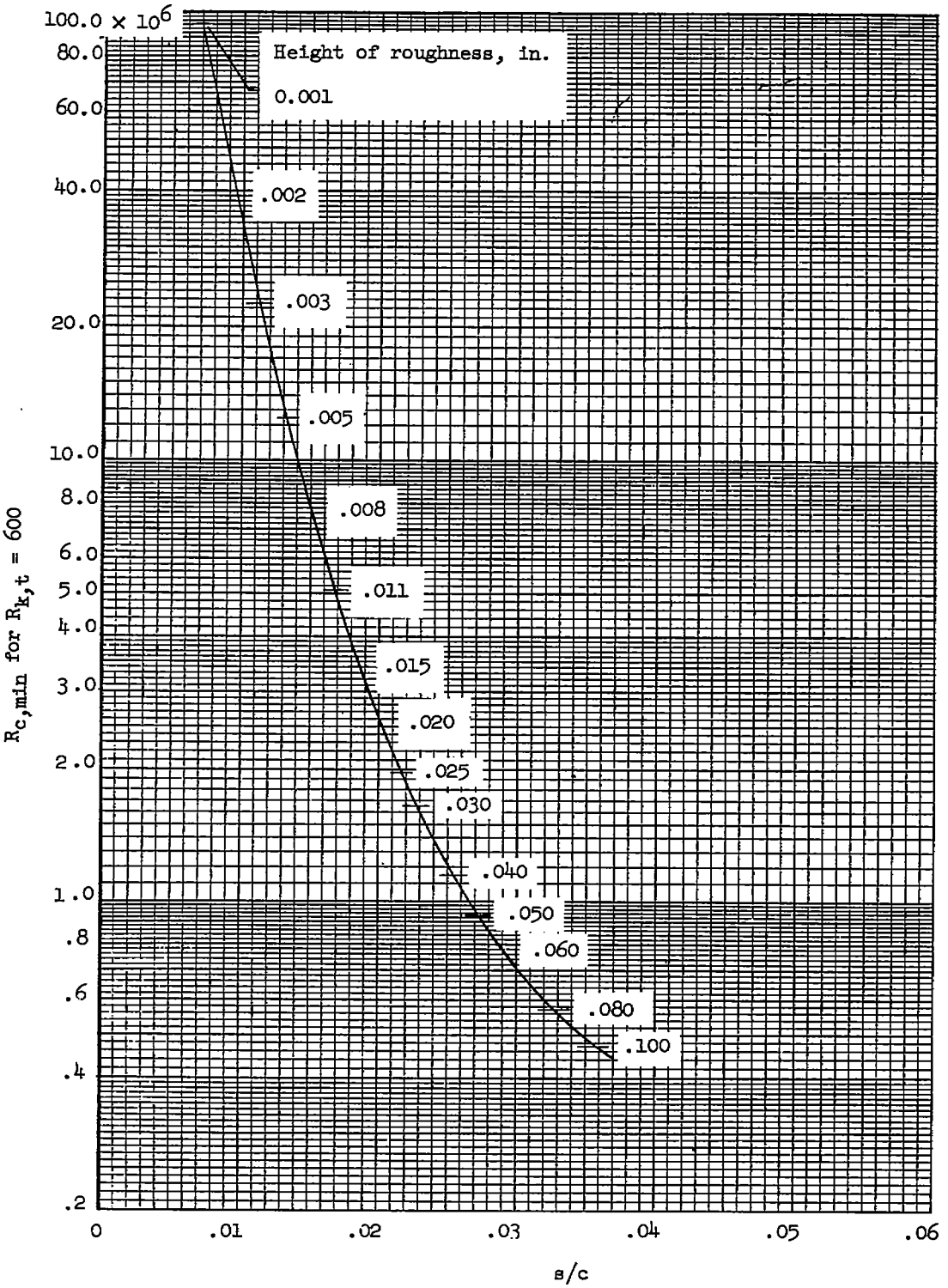


Figure 16.- The theoretical location, for various heights of roughness on an 85-inch-chord NACA $65_{(215)}$-114 airfoil section, at which, for a value of $R_{k,t}$ of 600, the airfoil Reynolds number $R_c$ will be a minimum.

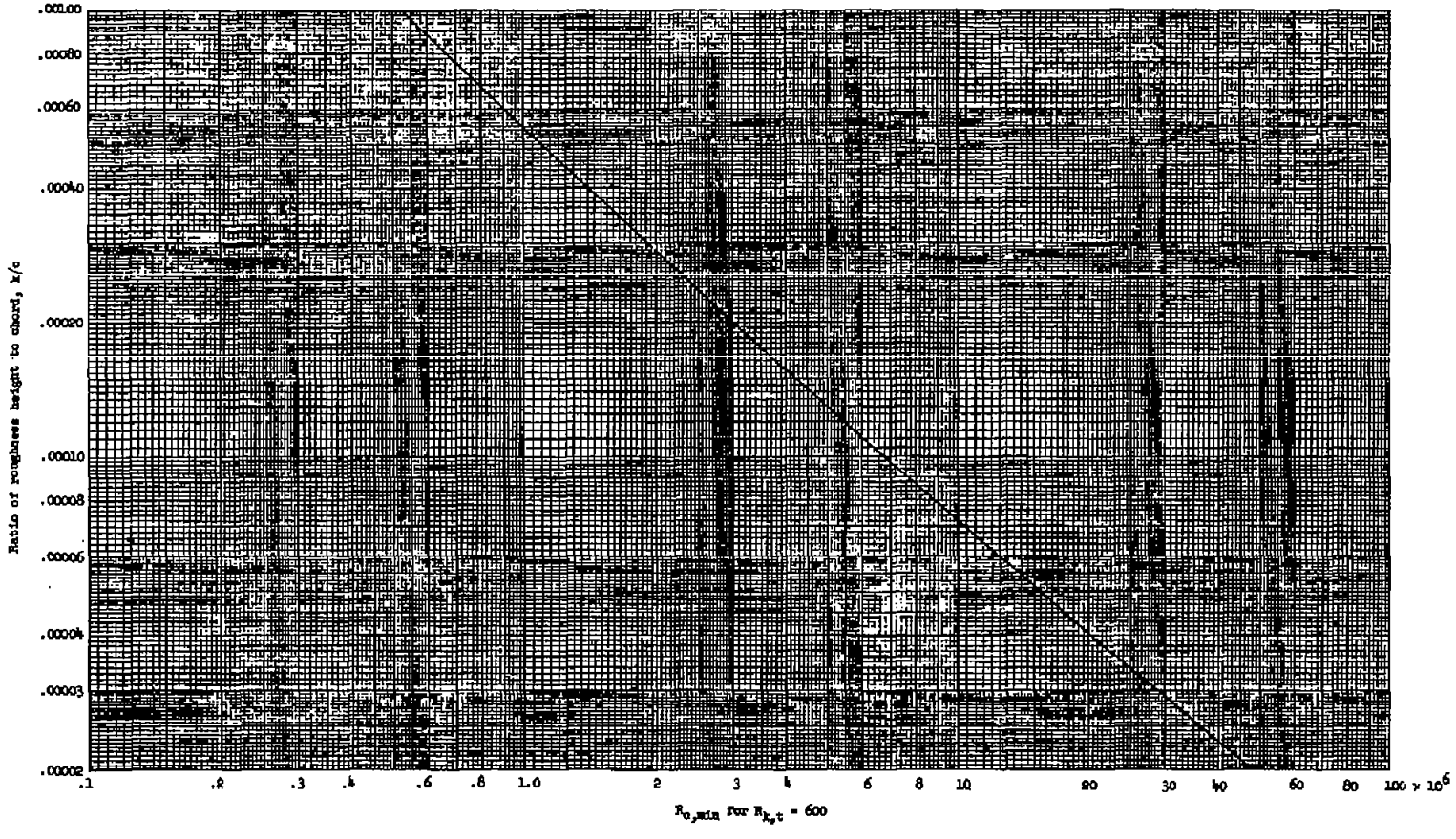


Figure 17.- Variation of the minimum airfoil Reynolds number $R_{c,min}$, for critical roughness Reynolds number $R_{k,t}$ of 600, with roughness height as calculated for an 85-inch-chord NACA $65_{(215)}$-114 airfoil section.

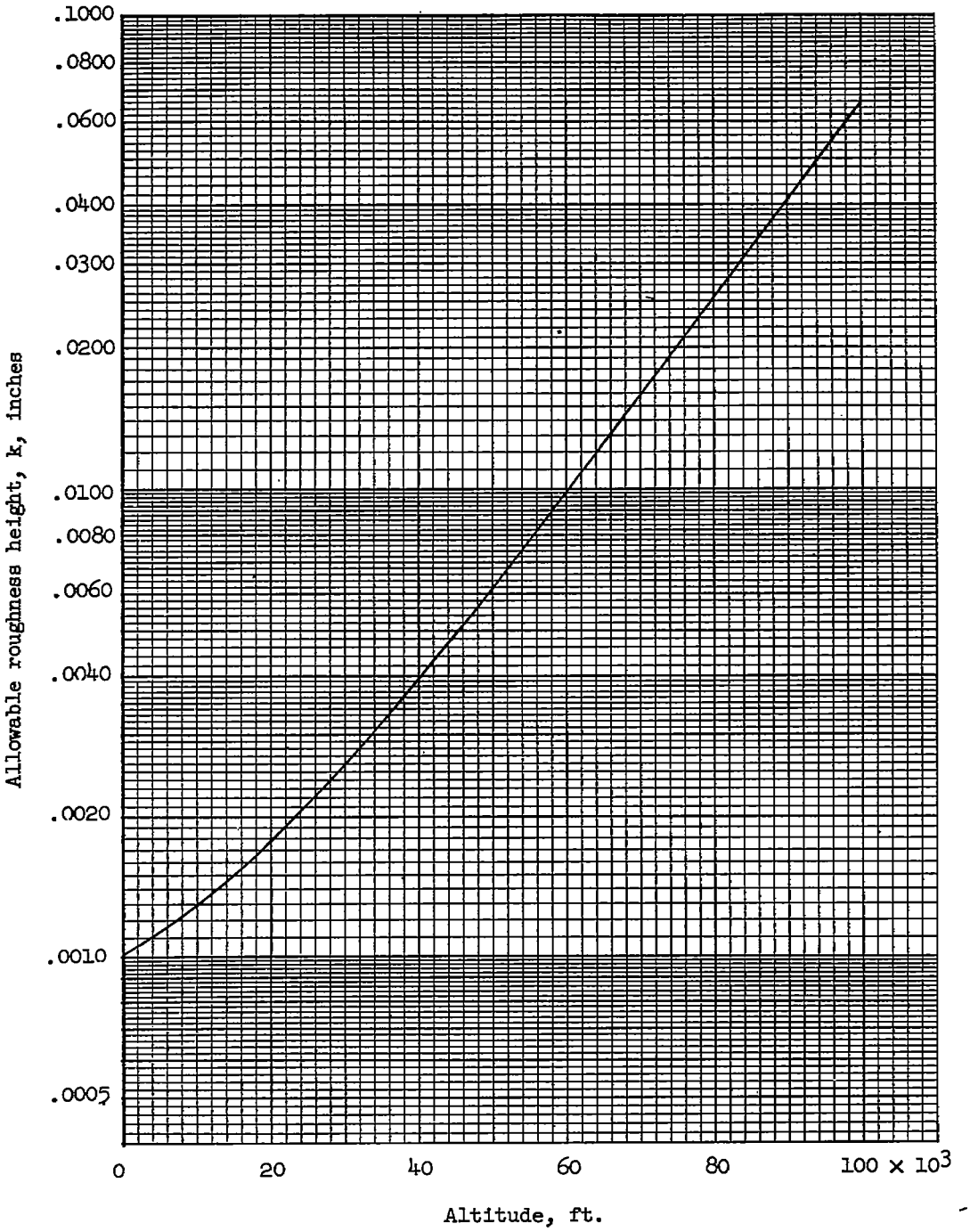


Figure 18.- Allowable roughness height for critical roughness Reynolds number, $R_{k,t}$ of 600, as function of altitude for Mach number of 1.0.

NACA - Langley Field, Va.